Classical Noise. VI. Noise in Self-Sustained Oscillators near Threshold*

ROBERT D. HEMPSTEAD† AND MELVIN LAX
Bell Telephone Laboratories, Murray Hill, New Jersey
(Received 28 March 1967)

Because of the relative narrowness of the threshold region, a general model for spectrally pure self-sustained oscillators (both classical and quantum, including gas lasers) can be reduced, in the threshold region, to a rotating-wave Van der Pol (RWVP) oscillator. By a scaling transformation, we reduce to the normalized RWVP oscillator which contains only one dimensionless parameter, a net pump rate p, which determines the operating point. The power spectra of phase and amplitude fluctuations and of amplitude (intensity) fluctuations in the normalized RWVP oscillator near threshold are calculated "exactly" by numerical Fokker-Planck methods. Using the appropriate scaling transformation, our results yield these power spectra for any oscillator of this general type. In particular, for gas lasers our results yield the one-sided Fourier transform of $\langle b^\dagger(t)b(0)\rangle$ (the spectrum) and of $\langle b^\dagger(0)b^\dagger(t)b(t)b(0)\rangle - \langle b^\dagger b\rangle^2$ (the intensity spectrum), where $b^\dagger$ and b are the creation and destruction operators for the radiation field. Except for intensity fluctuations just above threshold, the power spectra were found to be nearly Lorentzian, with half-widths at half power approximately equal to the lowest nonzero temporal eigenvalue of the Fokker-Planck equation. For intensity fluctuations above threshold, the second-lowest nonzero eigenvalue was found to yield a significant contribution to the power spectrum as well as the lowest nonzero eigenvalue. These two eigenvalues become nearly degenerate for operation well above threshold. Thus the intensity fluctuation spectrum is Lorentzian below and well above threshold, but more complex in the threshold region.

1. INTRODUCTION

CONSIDERABLE attention has been given recently to the Van der Pol oscillator as a semiclassical way of describing noise in masers and lasers.[1] It has been shown for the gas laser, and any other laser for which the atomic rate constants are fast compared to the photon-decay constants, that the electromagnetic-field operators have a Markoffian behavior and obey "Heisenberg" equations of the rotating-wave Van der Pol form[2,3] (RWVP) with quantum-noise sources that can be calculated from first principles.[4]

With the exception of the density-matrix treatment of Scully, Stephen and Lamb,[5] previous treatments have made quantum-mechanical calculations of diffusion coefficients and inserted them into a classical Fokker-Planck equation.[6] Even then, quasilinear approximations[7] have usually been used to avoid the solution of the Fokker-Planck equations that constitute the exact description of the classical random processes. For operation near the threshold of oscillation, quasilinear approximations are not valid, and one is forced to solve the Fokker-Planck equation.

Two different linearization schemes have been in common use. The mean-value method,[8] as explained in V, deals with the real and imaginary parts of the field as variables and replaces a nonlinear resistance by a mean value. For a laser, the population difference is not treated as a fluctuating variable, but replaced by a mean value.[8] In V, we suggested that this method should be adequate well below threshold, since the

* The work reported here overlaps appreciably the contents of a thesis submitted by R. D. H. to the Department of Electrical Engineering, Massachusetts Institute of Technology in September 1965, in partial fulfillment of the requirements for a Master of Science degree. Part of this work was previously presented at the New York meeting of the American Physical Society, Bull. Am. Phys. Soc. **11**, 111 (1966).

† Present address: Physics Department, University of Illinois, Urbana, Illinois.

[1] The importance of Van der Pol oscillators in describing lasers and laser noise has been emphasized by a number of authors: W. Lamb, Jr., Phys. Rev. **134**, A1429 (1964); H. A. Haus, J. Quant. Electron. **1**, 179 (1965); C. Freed and H. A. Haus, Appl. Phys. Letters **6**, 85 (1965); Phys. Rev. **141**, 287 (1966); J. A. Armstrong and A. W. Smith, Phys. Rev. Letters **14**, 68, 208 (1965); Phys. Letters **16**, 38 (1965); Phys. Rev. **140**, A155 (1965); H. Risken, Z. Physik **191**, 302 (1966).

[2] M. Lax and W. H. Louisell, J. Quant. Electron. **3**, 47 (1967). hereafter referred to as QIX (see Ref. 3).

[3] QIX stands for the ninth paper in a series of papers on quantum noise by M. Lax: QI: Phys. Rev. **109**, 1921 (1958); QII: **129**, 2342 (1963); QIII: J. Phys. Chem. Solids **25**, 487 (1964); QIV: Phys. Rev. **145**, 110 (1966); QV: in *Physics of Quantum Electronics*, edited by P. L. Kelley, B. Lax, and P. E. Tannenwald (McGraw-Hill Book Company, Inc., New York, 1966) p. 735; QVI: (with D. R. Fredkin) (to be published); QVII: J. Quant. Electron. **3**, 37 (1967); QVIII: H. Cheng and M. Lax in *Quantum Theory of the Solid State*, edited by Per-Olav Lowdin (Academic Press Inc., New York, 1966), p. 587; QIX: (with W. H. Louisell), J. Quant. Electron. **3**, 47 (1967); QX: Phys. Rev. **157**, 213 (1967); QXI: (to be published); QXII: with W. H. Louisell (to be published).

[4] See QIV.

[5] M. Scully, W. E. Lamb, Jr., and M. J. Stephen, in *Physics of Quantum Electronics*, edited by P. L. Kelley, B. Lax, and P. E. Tannenwald (McGraw-Hill Book Company, Inc., New York, 1966), p. 759; M. Scully and W. E. Lamb, Jr., Phys. Rev. Letters **16**, 853 (1966).

[6] H. Haken, Z. Physik **190**, 327 (1966); H. Sauermann, *ibid.* **188**, 480 (1965); **189**, 312 (1966); H. Risken, C. Schmid, and W. Weidlich, Phys. Letters **20**, 489 (1966).

[7] For a general discussion of quasilinear methods see I; for a quasilinear treatment of self-sustained oscillators see V, the first and fifth papers in the series on classical noise by M. Lax: I: Rev. Mod. Phys. **32**, 25 (1960); II: J. Phys. Chem. Solids **14**, 248 (1960); III: Rev. Mod. Phys. **38**, 359 (1966); IV: **38**, 541 (1966); V: Bull. Am. Phys. Soc. **11**, 111 (1966) and Phys. Rev. **160**, 290 (1967).

[8] W. G. Wagner and G. Birnbaum, J. Appl. Phys. **32**, 1185 (1961); D. E. McCumber, Phys. Rev. **130**, 675 (1962); A. L. Schawlow and C. H. Townes, *ibid.* **112**, 1940 (1958); J. A. Fleck, Jr., J. Appl. Phys. **34**, 2997 (1963); R. V. Pound, Ann. Phys. (N. Y.) **1**, 24 (1957); M. P. W. Strandberg, Phys. Rev. **106**, 617 (1957); J. Weber, Rev. Mod. Phys. **31**, 681 (1959); W. H. Wells, Ann. Phys. (N. Y.) **12**, 1 (1961); G. Kemeny, Phys. Rev. **133**, A69 (1964); H. Risken, Z. Physik **180**, 150 (1964).

nonlinear term, although crudely treated, is small compared to the linear term which then is dominant in determining the over-all response. The second linearization scheme[9] used the amplitude and phase of the field variables, and makes a quasilinear approximation in the amplitude only. This method used, for example, by the Haken School,[6] and by us[3] in QV, was recognized[7] in V to be valid only well above threshold.

The present paper supplies exact numerical solutions of the Fokker-Planck equation. In the region near threshold, (power output within a factor of 10 of the threshold value), we demonstrate that neither linearization scheme is sufficiently accurate. We also demonstrate our previous conjectures that the mean-value method is adequate well below threshold, and that the quasilinear method becomes increasingly accurate well above threshold. These qualitative conclusions are also suggested by Risken's[10] variational treatment of the lowest eigenfunctions of the Fokker-Planck operator.

The spectrum of our oscillator (for a laser, this is the Fourier transform of $\langle b^\dagger(t)b(0)\rangle$, where $b^\dagger$ and b are creation and destruction operators for the harmonic oscillator describing the field) is shown to be nearly Lorentzian. Thus the linewidth of this noise spectrum will be determined, as demonstrated below, primarily by the lowest eigenvalue Λ_p (p for phase) of the Fokker–Planck operator for the restricted set of eigenfunctions which vary as $\exp(i\phi)$, that determine the spectrum of phase ϕ (and amplitude $r=|b|$) fluctuations contained in $\langle r(t)\exp[i\phi(t)]r(0)\exp[-i\phi(0)]\rangle$.

As is well known,[9] the linewidth Λ_p is inversely proportional to the power. The proportionality constant obtained by the mean-value method (see for example the Schawlow-Townes[8] formula) is twice that obtained by the quasilinear method.[9] Our present numerical results for Λ_p display the transition from the Schawlow-Townes formula, below threshold, to the quasilinear formula above threshold.

The spectrum of intensity (pure amplitude) fluctuations [for a laser this is the Fourier transform of $\langle b^\dagger(0)b^\dagger(t)b(t)b(0)\rangle$] is also demonstrated to be nearly Lorentzian except for a region just above threshold. In the Lorentzian region, the linewidth is determined by the lowest nonvanishing eigenvalue Λ_a for the phase-independent solutions of the Fokker-Planck equation. The quasilinear estimate of this linewidth, as well as Λ_a, display a minimum *near* threshold in agreement with experimental measurements of amplitude fluctuations.[11]

The basis for our ability to apply the results of a classical random problem to the laser, which is a quantum random problem, is given in QIX [3] by Lax and Louisell, who have set up a dynamical correspondence between the density matrix of the electromagnetic field $\rho(b, b^\dagger, t)$ and an associated classical function $\bar{p}^{(a)}(\beta, \beta^*, t)$.[12] The correspondence is simply that the density operator is to be obtained from its associated classical function by replacing β by b and β^* by $b^\dagger$ obeying the antinormal ordering rule: all $b^\dagger$'s are to be placed to the *right*, and all b's are to be placed to the *left*. The *classical* average of any classical function $\bar{M}^{(n)}(\beta, \beta^*, t)$ of β and β^* over the classical probability distribution $\bar{p}^{(a)}(\beta, \beta^*, t)$ corresponds to the *quantum* average of the quantum operator $M(b, b^\dagger, t)$ obtained from $\mathrm{M}^{(n)}(\beta, \beta^*, t)$ by replacing β by b and β^* by $b^\dagger$ and obeying the *normal* ordering rule: All $b^\dagger$'s are to be placed to the *left*, and all b's are to be placed to the *right*. (The relation between our ordering procedure and the classical correspondences, adopted by other authors are discussed,[12–15] with references, in QIX and QX.)

In QXII, Lax and Louisell obtain a Fokker–Planck equation for $\bar{p}^{(a)}(\beta, \beta^*, N_1, N_2, t)$ where N_1 and N_2 are populations of the lower and upper laser levels, respectively.[16] For a laser in which all of the atomic response rates are fast compared to the photon rates, an adiabatic approximation for the population variables N_1 and N_2 yields a Fokker-Planck equation for $\bar{p}^{(a)}(\beta, \beta^*, t)$. In Appendix A we quote the Langevin process appropriate to this Fokker-Planck process. Treatment of the nonlinearity by an expansion in $|\beta|^2$ is shown in Appendix A (a) to lead to the Van der Pol oscillator, (b) to be valid from zero photons up to a number of photons greatly exceeding the number at threshold.

In Appendix B we consider a classical circuit model of an oscillator to demonstrate that the reduction to

[9] See for example, W. A. Edson, Proc. IRE **48,** 1454 (1960); J. A. Mullen, *ibid.* **48,** 1467 (1960); M. E. Golay, *ibid.* **48,** 1473 (1960); P. Grivet and A. Blaquiere, in *Optical Physics* (John Wiley & Sons, Inc., New York, 1963), p. 69. See also the many relevant papers in P. I. Kuznetsov, R. I. Stratanovitch, and V. I. Tikhonov, *Non-Linear Transformations of Stochastic Processes* (Pergamon Press, Oxford, England 1965).

[10] H. Risken, Z. Physik **191,** 302 (1966).

[11] C. Freed and H. A. Haus, Phys. Rev. **141,** 287 (1966); J. A. Armstrong and A. W. Smith, *ibid.* **140,** A155 (1965); F. T. Arecchi, Phys. Rev. Letters **15,** 912 (1965); F. T. Arecchi, A. Berne, and P. Bulamacchi, *ibid.* **16,** 32 (1966); W. Martienssen and F. Spiller, Phys. Rev. **145,** 285 (1966). See also Ref. 1.

[12] We have established in QIX that, at any one time, our "classical" function $\bar{p}^{(a)}(\beta, \beta^*, t)$ is identical (aside from a factor π) to the $P(\beta)$ function of Glauber (see Ref. 13), Sudarshan (see Ref. 14) and Klauder (see Ref. 15). Our procedure is dynamical in that we calculate $P(\beta, t)$ using a Fokker-Planck equation description of the field plus reservoirs rather than using a conjectured steady state $P(\beta)$ plus free field dynamics (Refs. 13–15). A demonstration of the full equivalence between averages of time-ordered, normally-ordered operators in the quantum problem and ordinary averages in the associated "classical" problem is established in QXI. See also M. Lax, in *Brandeis Summer Institute in Theoretical Physics Lecture Notes* (Gordon and Breach, Science Publishers, Inc., New York, to be published), Chap. 11.

[13] R. J. Glauber, Phys. Rev. **130,** 2529 (1963); **131,** 2766 (1963).

[14] E. C. G. Sudarshan, Phys. Rev. Letters **10,** 277 (1963); *Proceedings of the Symposium on Optical Masers* (John Wiley and Sons, Inc., New York 1963), p. 45.

[15] See also J. R. Klauder, J. Math. Phys. **4,** 1055 (1963); **5,** 177, 878 (1964) and Phys. Rev. Letters **16,** 534 (1966). For an excellent review, see L. Mandel and E. Wolf, Rev. Mod. Phys. **37,** 231 (1965).

[16] See also M. Lax, in *Dynamical Processes in Solid State Optics* (W. A. Benjamin Inc., New York, 1967), p. 195. A description in terms of the field, N_1, and N_2 is appropriate when the population equilibration times are comparable (or slower) than those of the field. If N_1 empties rapidly, a simpler description in terms of $\rho(b, b^\dagger, N_2, t)$ is possible as shown in QX.

Van der Pol form over a broad region including threshold is valid for nearly all "well-designed" oscillators. We define a well-designed oscillator to be one whose output is sinusoidal rather than periodic, and whose output is large compared to thermal noise in a similar circuit in which all resistances are positive.

In Appendices A and B, we show that it is possible to scale our amplitude variable and the time in such a way as to eliminate all parameters but a single dimensionless parameter p. For a laser, p is proportional to the excess of the pump rate over the threshold pump rate. Our scaled Langevin equations are just those of the normalized rotating wave Van der Pol (NRWVP) oscillator equations studied in V[7] by quasilinear methods.

We can, therefore, for a broad class of oscillators start with the NRWVP-oscillator Langevin equations. The corresponding Fokker-Planck equation is derived using the real and imaginary parts of the complex amplitude of the oscillator as variables. Since we are interested in phase and amplitude noise, a transformation to the magnitude and phase of the complex amplitude is made in Sec. 3. In order to reduce the number of variables in the Fokker-Planck equation, certain integrals over the phase variable are performed since it is only these integrals over the probability distribution which are needed. In Sec. 5 we obtain the steady-state amplitude probability distribution, which is used to obtain the dependence of the scaled photon number (or scaled intensity) $\bar{p}$ on our dimensionless pump parameter p. By taking the one-sided Fourier transform of the equation resulting from the phase integrals over the Fokker-Planck equation, we obtain an *ordinary* differential equation for a Green's function whose moments give directly the power spectra of phase and amplitude fluctuations and of amplitude (intensity) fluctuations.

This linear differential equation was numerically integrated and the power spectra for operation near threshold were obtained. Appendix C is a discussion of the boundary conditions used in this numerical integration.

These power spectra were found to be very nearly Lorentzian for frequencies less than, and of the order of, the half-width at half power. This suggested the usefulness of the usual expansion[17] of the conditional probability distribution in the eigenfunctions corresponding to the temporal eigenvalues of the Fokker-Planck equation, since a nearly Lorentzian power spectrum implies that the contribution of the lowest nonzero eigenvalue is dominant. The half-widths at half power of these power spectra were found to be given by the lowest nonzero eigenvalues. We compare the exact results to what has been called an intelligent quasilinear approximation in V.

We want to emphasize that our exact results need only be scaled by the scaling factors given in Appendix A to give the results for a gas laser, and by the scaling factors in Appendix B to give the results for a large class of oscillators.

The present work differs from that of previous authors in the following respects:

(1) From the direct correspondence between the density matrix and a classical probability distribution established in QIX, the *quantum-mechanical spectrum* and moments are precisely calculated in terms of the *corresponding classical spectra* and moments.

(2) All results and figures shown here were obtained by numerical integration of the appropriate Fokker–Planck equations and are *essentially exact.*

(3) A *direct* calculation is made of the power spectra of phase and amplitude fluctuations and of amplitude (intensity) fluctuations by Green's-function methods.

(4) The results are checked by eigenfunction methods. For this latter purpose, numerical computations were made of the ten lowest nonzero eigenvalues and their corresponding eigenfunctions. This was done both for the usual spectrum (phase and amplitude fluctuations) and for intensity fluctuations for values of p covering the threshold region. Risken[10] estimated (by variational methods only) the lowest eigenvalues Λ_p Λ_a in these two series.

(5) The Scully-Lamb procedure[5] (even if they performed a time scaling) would retain two parameters since the discrete photon number n cannot be scaled without approximation. Our scaling down to a single parameter p permits numerical solution of differential equations exploring a one-dimensional parameter space. The Scully-Lamb procedure, as presently used, must perform the much greater labor of exploring a two-parameter space. Moreover, for each point in that space, they solve not a single second-order differential equation but an $N\times N$ system of simultaneous equations where N must be large compared to the mean number of photons.

2. THE LANGEVIN AND FOKKER-PLANCK EQUATIONS

Our remarks of the preceding section establish the appropriateness of beginning with the "reduced" Langevin equations for the normalized rotating-wave Van der Pol oscillator, V [Eq. (9.4)].[17]

$$dx/dt=[p-(x^2+y^2)]x+F_x(t), \tag{2.1}$$

$$dy/dt=[p-(x^2+y^2)]y+F_y(t), \tag{2.2}$$

where the Langevin forces F_x and F_y represent Gaussian white-noise sources with the following moments:

$$\langle F_x\rangle=\langle F_y\rangle=0,$$

$$\langle F_x(t)\,F_x(u)\rangle=\langle F_y(t)\,F_y(u)\rangle=2\delta(t-u),$$

$$\langle F_x(t)\,F_y(u)\rangle=\langle F_y(t)\,F_x(u)\rangle=0. \tag{2.3}$$

[17] See M. Lax, in *Brandeis Summer Institute in Theoretical Physics Lecture Notes* (Gordon and Breach Science Publishers Inc., New York, to be published).

Since these Langevin forces are assumed Gaussian[18]

$$\langle F_1(t_1)\cdots F_n(t_n)\rangle^L=0 \quad \text{for} \quad n>2; \qquad (2.4)$$

where $\langle\ \rangle^L$ denotes a linked average[19,20] and $F_i(t_i)=F_x(t_i)$ or $F_y(t_i)$.

Because our noise sources are white, this process is Markoffian and therefore the conditional probability $P(x, y, t \mid x_0, y_0, t_0)$ obeys a generalized Fokker-Planck equation [IV(5.13)]:

$$\frac{\partial P}{\partial t}=\sum_{n=1}^{\infty}(-1)^n(\partial/\partial \mathbf{a})^n:[\mathbf{D}_n(\mathbf{a}, t)P(\mathbf{a}, t)], \qquad (2.5)$$

where $\mathbf{a}=a_1, a_2\cdots$ are the set of random variables—in this case x and y—and the diffusion coefficients $\mathbf{D}_n$ are defined by

$$n!\mathbf{D}_n(\mathbf{a}, t)$$

$$=\lim_{\Delta t\to 0}(\Delta t)^{-1}\int P(\mathbf{a}', t+\Delta t \mid \mathbf{a}, t)(\mathbf{a}'-\mathbf{a})^n d\mathbf{a}', \qquad (2.6)$$

where $\mathbf{D}_n$ has n (suppressed) subscripts, and : is a shorthand notation which tells us to multiply corresponding terms, e.g., the moment of $(a_1'-a_1)^2(a_2'-a_2)$ would be written D_{112} and the corresponding term in the Fokker-Planck equation would be $(-1)^3(\partial^3/\partial^2 a_1\partial a_2)[D_{112}P]$. The $n=1$ and $n=2$ terms correspond to the ordinary Fokker-Planck equation, and the Gaussian property of our Langevin forces guarantees that all higher-order diffusion coefficients for our process vanish.[21]

To obtain the first- and second-order diffusion coefficients,[22] we must write the Langevin equations as integral equations:

$$\Delta x\equiv x(t+\Delta t)-x(t)$$

$$=\int_t^{t+\Delta t}\{[p-\rho(s)]x(s)+F_x(s)\}ds, \qquad (2.7)$$

where $\rho(s)\equiv[x(s)]^2+[y(s)]^2$ and similarly for Δy. We now iterate these integral equations by first replacing $x(s)$, and $y(s)$ inside the integral by $x(t)$ and $y(t)$, respectively, yielding the first approximation:

$$(\Delta x)_1=[p-\rho(t)]x(t)\Delta t+\int_t^{t+\Delta t}F_x(s)ds \qquad (2.8)$$

and similarly for $(\Delta y)_1$.

From the definition of the diffusion coefficients $\mathbf{D}_n$, Eq. (2.6), we see that Δx and Δy need be calculated to only first order in Δt. Care must be exercised, however, since means of products of the Langevin forces are singular, hence nominally higher-order terms may contain a contribution which is first order in Δt. To resolve this question, we must examine

$$\int_t^{t+\Delta t}ds_1\cdots\int_t^{t+\Delta t}ds_m\int_t^{t+\Delta t}ds_1'\cdots\int_t^{t+\Delta t}ds_n'$$

$$\times\langle F_x(s_1)\cdots F_x(s_m)F_y(s_1')\cdots F_y(s_n')\rangle. \qquad (2.9)$$

Since the Langevin forces are Gaussian random variables

$$\langle F_x(s_1)\cdots F_x(s_m)F_y(s_1')\cdots F_y(s_n')\rangle$$

vanishes if $(m+n)$ is odd and is equal to

$$\langle F_x(s_1)F_x(s_2)\rangle\langle F_x(s_3)F_x(s_4)\rangle\cdots\langle F_y(s_{n-1}')F_y(s_n')\rangle$$

+all other pair decompositions

if $(m+n)$ is even. Thus, our term (2.9) vanishes if $(m+n)$ is odd and is of order $(m+n)/2$ in Δt if $(m+n)$ is even. Hence, only products of two Langevin forces yield terms which are first order in Δt. Thus, in general,[21] we would have to iterate once more to calculate $(\Delta x)_2$, the contribution to Δx of second order, in the random forces. Because our Eqs. (2.7) have a simple structure in which the random forces are not multiplied by random variables, no such second-order terms arise.[23] Therefore, $(\Delta x)_1$ and $(\Delta y)_1$ are correct to first order in Δt, and we can calculate the drift coefficients A_x and A_y:

$$A_x\equiv D_x=\langle(\Delta x)_1\rangle/\Delta t=[p-x^2-y^2]x, \qquad (2.10)$$

$$A_y\equiv D_y=\langle(\Delta y)_1\rangle/\Delta t=[p-x^2-y^2]y. \qquad (2.11)$$

We have used the vanishing of $\langle F_x\rangle$ and $\langle F_y\rangle$ which follows from the definition of Langevin forces. In order to calculate the diffusion coefficients, D_{xx} and D_{yy}, we must square $(\Delta x)_1$, which gives us a nominally second-order expression but contains a product of Langevin forces of the type mentioned above:

$$D_{xx}=\frac{1}{2}\frac{\langle(\Delta x)_1^2\rangle}{\Delta t}$$

$$=\frac{1}{2\Delta t}\int_t^{t+\Delta t}ds\int_t^{t+\Delta t}ds'\langle F_x(s)F_x(s')\rangle=1. \qquad (2.12)$$

Similarly,

$$D_{yy}=1. \qquad (2.13)$$

The diffusion coefficient D_{xy} vanishes as a result of the

---

[18] In Sec. 6 of QIV, the assumption that the Langevin forces are Gaussian is shown to be a good approximation for lasers.

[19] Linked moments, also known as Thiele semi-invariants or cumulants (see Ref. 20) are defined by III (6.8) or IV (2.5). We rewrite the latter in the form

$$\langle\exp\int\mathbf{q}(s)\cdot\mathbf{F}(s)ds-1\rangle^L=\ln\langle\exp\int\mathbf{q}(s)\cdot\mathbf{F}(s)ds\rangle$$

and expand both sides in powers of $\mathbf{q}(s)$ and compare corresponding terms to obtain the definitions of the linked moments of first, second, third, etc. order. For use in (2.4), we must regard $\mathbf{q}(s)$ as a two-component vector function so that $\mathbf{q}(s)\cdot\mathbf{F}(s)\equiv q_x(s)F_x(s)+q_y(s)F_y(s)$.

[20] R. Kubo, J. Phys. Soc. Japan **17**, 1100 (1962).

[21] See IV, Sec. 3.

[22] We repeat here, for our process, the method of IV, Sec. 3 for determining the diffusion coefficients.

[23] Such products of random variables times forces would have appeared if we had worked in circular variables r, ϕ instead of Cartesian variables x, y. Such extra terms appear in a different way [see the last term of (3.1)] when we transform from rectangular to circular coordinates.

absence of correlation between the Langevin forces F_x and F_y:

$$D_{xy}=\frac{1}{2}\frac{\langle(\Delta x)_1(\Delta y)_1\rangle}{\Delta t}$$
$$=\frac{1}{2\Delta t}\int_t^{t+\Delta t}ds\int_t^{t+\Delta t}ds'\langle F_x(s)F_y(s')\rangle=0. \quad (2.14)$$

All higher-order diffusion coefficients are computed from $\langle(\Delta x)_1{}^m(\Delta y)_1{}^n\rangle$ for $m+n>2$, which will be a sum of terms of the form

$$(\Delta t)^{i+j}\int_t^{t+\Delta t}ds_1\cdots\int_t^{t+\Delta t}ds_{m-i}\int_t^{t+\Delta t}ds_1'\int_t^{t+\Delta t}ds_{n-j}'$$
$$\times\langle F_x(s_1)\cdots F_x(s_{m-i})F_y(s_1')\cdots F_y(s_{n-j}')\rangle$$
$$0\leq i\leq m;\quad 0\leq j\leq n \quad (2.15)$$

From our discussion of the time integrals, we see that $\langle(\Delta x)_1{}^m(\Delta y)_1{}^n\rangle$ is of order $\frac{1}{2}(m+n)$ in Δt for $(m+n)$ even and of order $\frac{1}{2}(m+n+1)$ for $(m+n)$ odd. Hence, all higher-order diffusion coefficients vanish, and our process is a Fokker-Planck process.

Our conclusion is that the conditional probability $P(x, y, t\,|\,x_0, y_0, t_0)$ satisfies the following Fokker-Planck equation:

$$\frac{\partial P}{\partial t}=-\frac{\partial}{\partial x}[(p-x^2-y^2)xP]-\frac{\partial}{\partial y}[(p-x^2-y^2)yP]$$
$$+\frac{\partial^2P}{\partial x^2}+\frac{\partial^2P}{\partial y^2}, \quad (2.16)$$

3. TRANSFORMATION TO POLAR COORDINATES

The transformation to polar coordinates $a\equiv x-iy=re^{-i\phi}$ is a natural consequence of our interest in amplitude noise as well as fluctuations in $(x-iy)$. To accomplish this transformation, we use the transformation laws for the drift and diffusion coefficients given in Eqs. IV(3.27) and IV(3.28):

$$a_i'=a_i'(\mathbf{a}, t),$$
$$D_{ij}'=(\partial a_i'/\partial a_k)(\partial a_j'/\partial a_l)D_{kl},$$
$$A_i'=\partial a_i'/\partial t+(\partial a_i'/\partial a_k)A_k+(\partial^2 a_i'/\partial a_m\partial a_n)D_{mn}; \quad (3.1)$$

and preservation of normalization requires that

$$P'(\mathbf{a}', t)\equiv JP(\mathbf{a}, t), \quad (3.2)$$

where

$$J\equiv\det(\partial a_i/\partial a_j') \quad (3.3)$$

is the Jacobian of the transformation.

Using the above transformation laws, the Fokker-Planck equation in polar coordinates is found to be

$$\frac{\partial P}{\partial t}=\frac{\partial}{\partial r}[(r^3-pr-r^{-1})P]+\frac{\partial^2P}{\partial r^2}+\frac{1}{r^2}\frac{\partial^2P}{\partial\phi^2}. \quad (3.4)$$

4. INTEGRATION OVER THE PHASE VARIABLE

In order to calculate the spectrum of phase and amplitude fluctuations

$$S_p(\omega)=2\int_{-\infty}^{\infty}\langle a^*(t)a(0)\rangle e^{-i\omega t}dt, \quad (4.1)$$

where $a=x-iy$, and of amplitude (intensity) fluctuations,

$$S_a(\omega)=2\int_{-\infty}^{\infty}[\langle a^*(0)a^*(t)a(t)a(0)\rangle-\langle a^*a\rangle^2]e^{-i\omega t}dt, \quad (4.2)$$

we must perform an integration over the phases. This suggests that it is not necessary to compute P, but only the simpler quantities:

$$\hat{R}(r, t\,|\,r_0, 0; \lambda)$$
$$=\int d(\phi-\phi_0)\exp[+i\lambda(\phi-\phi_0)]P(r, \phi, t\,|\,r_0, \phi_0, 0) \quad (4.3)$$

with $\lambda=1$ for S_p (phase) and $\lambda=0$ for S_a (amplitude). For $\lambda=0$, $\hat{R}$ will be the conditional probability distribution of the amplitude r.

The equation satisfied by $\hat{R}$ may be derived from the Fokker-Planck equation by recognizing that $\hat{R}$ is the Fourier transform of P; therefore P may be expressed as the inverse transform of $\hat{R}$. Substituting this expression for P into the Fokker-Planck equation yields

$$\int d\lambda\exp[-i\lambda(\phi-\phi_0)]\frac{d\hat{R}}{\partial t}$$
$$=\int d\lambda\exp[-i\lambda(\phi-\phi_0)]\left[H_r-\frac{\lambda^2}{r^2}\right]\hat{R}, \quad (4.4)$$

where the differential operator H_r is defined to be

$$H_r\equiv\partial/\partial r[r^3-pr-r^{-1}]+(\partial^2/\partial r^2). \quad (4.5)$$

The inverse transform of this equation yields the desired equation for $\hat{R}$.

$$\partial\hat{R}/\partial t=H_r\hat{R}-(\lambda^2/r^2)\hat{R}. \quad (4.6)$$

Notice, that by this procedure, we have eliminated the phase variable from our Fokker-Planck equation. The new "probability" distribution $\hat{R}(r, t\,|\,r_0, t_0; \lambda)$ is the conditional probability distribution of the amplitude r when $\lambda=0$ and is an unnormalized distribution for r when $\lambda=1$.[24]

5. STEADY-STATE AMPLITUDE PROBABILITY DISTRIBUTION

The steady-state amplitude probability distribution, $P(r)$, will be used to compute $\bar{p}\equiv\langle r^2\rangle$ as a function of

[24] See III for a discussion of the usefulness of defining an unnormalized probability distribution in treating nonlinear Markoff processes.

the dimensionless pump parameter p. This functional dependence, shown in Fig. 1, allows the experimenter to determine the value of our pump parameter p for his oscillator by measuring the power output and using the appropriate scaling laws. We also use $P(r)$ in Sec. 6 for the calculation of the power spectra, and in the eigenfunction expansion of Sec. 7.

As stated in Sec. 4, by setting $\lambda=0$ in Eq. (4.6), we obtain an equation for the conditional probability of the amplitude. Using the stationary property

$$\lim_{(t-t_0)\to\infty} P(r, t \mid r_0, t_0) = P(r),$$

and taking this limit on both sides of Eq. (4.6), we obtain an equation for $P(r)$.

$$0=(\partial/\partial r)\{[r^3-pr-r^{-1}]P+(\partial P/\partial r)\}=-\partial J/\partial r. \tag{5.1}$$

If we regard

$$J\equiv[r^3-pr-r^{-1}]P+(\partial P/\partial r) \tag{5.2}$$

as a probability current, then (5.1) describes a conservation of probability. The boundary condition $J=0$ is a detailed-balance condition which is obeyed by our process.[25,26] With this boundary condition we obtain

$$P(r)=r\exp(-\tfrac{1}{4}r^4+\tfrac{1}{2}pr^2)\Big/\int_0^\infty r\exp(-\tfrac{1}{4}r^4+\tfrac{1}{2}pr^2)\,dr. \tag{5.3}$$

Since the experimenter measures the power output of the laser (or any other oscillator), we must relate

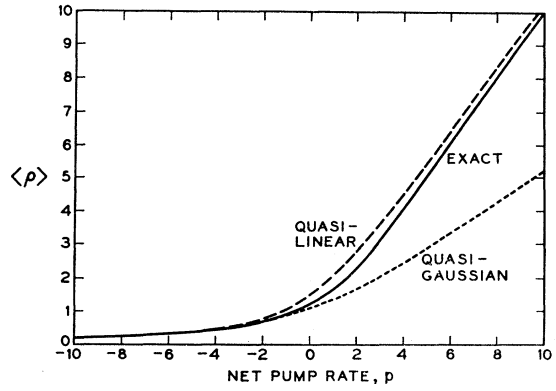

FIG. 1. The mean amplitude squared (intensity) $\bar{p}\equiv\langle\,|\,a\,|^2\rangle$ for the NRWVP oscillator is plotted as a function of the pump parameter p. For a laser, $\bar{p}$ is the normalized mean number of photons $\langle b^\dagger b\rangle/\xi^2$, where ξ^2 is defined by Eq. (A.13). The solid curve gives our exact values. The upper dashed curve is the quasi-linear approximation, which was obtained as usual from $\langle A(\rho)\rangle\cong A(\langle\rho\rangle)=0$ and yields $\rho_{QL}=\frac{1}{2}[p+(p^2+8)^{1/2}]$. Below threshold, the Gaussian nature of the radiation field suggests $\langle\rho^2\rangle=2\langle\rho\rangle^2$ which yields $\rho_{QG}=\frac{1}{4}[p+(p^2+16)^{1/2}]$, an excellent approximation below threshold but a poor one above (lower dashed curve).

[25] In general J need not be zero, and detailed balance is not obeyed. See IV, Sec. 4 for an example in which $J\neq0$. For further discussion of detailed balance see III, Sec. 7B, and Ref. 17, Chap. 8.

[26] For the relation between time-reversal, detailed balance and orthogonality, see Ref. 17, Chap. 8.

TABLE I. Mean intensity $\bar{p}=\langle\,|\,a\,|^2\rangle$ and total intensity fluctuation $\langle(\Delta\rho)^2\rangle=\langle\rho^2\rangle-(\bar{p})^2$ for NRWVP oscillator versus net pump parameter p.

p	$\bar{p}$	$\langle(\Delta\rho)^2\rangle$
−10	0.1927006	0.03586023
− 9	0.2124018	0.04326977
− 8	0.2363771	0.05310890
− 7	0.2660998	0.06649266
− 6	0.3037539	0.08521009
− 5	0.3526810	0.1122112
− 4	0.4181610	0.1524975
− 3	0.5088015	0.2147167
− 2	0.6389659	0.3137907
− 1	0.8327063	0.4738940
0	1.128379	0.7267611
1	1.577956	1.088010
2	2.225271	1.498711
3	3.060490	1.815462
4	4.010358	1.958462
5	5.001089	1.994553
6	6.000070	1.999583
7	7.000003	1.999981
8	8.000000	2.000000
9	9.000000	2.000000
10	10.000000	2.000000

the power output $\bar{p}\equiv\langle r^2\rangle$ to our dimensionless pump parameter p. Integrating $r^2P(r)$, numerically using (5.3), we obtain $\bar{p}$ as a function of p in the region near threshold.[27] The results are shown in Fig. 1 and Table I.

The integrated spectrum of phase and amplitude fluctuations using (4.1) can be written

$$\frac{1}{2}\int_{-\infty}^{\infty}\frac{S_p(\omega)\,d\omega}{2\pi}=\langle a^*(0)a(0)\rangle=\langle\rho\rangle=\bar{p} \tag{5.4}$$

if we use

$$\int_{-\infty}^{\infty}\frac{\exp(i\omega t)\,d\omega}{2\pi}=\delta(t).$$

Similarly, the total amplitude noise, using (4.2), can

[27] The results for $\bar{p}=\langle\rho\rangle$ were also checked by expressing $\langle\rho\rangle$ in terms of error integrals

$$\langle\rho\rangle=p+2^{-1/2}\left[e^{p^2/4}\int_{-p/\sqrt{2}}^{\infty}e^{-t^2/2}dt\right]^{-1}.$$

For $p<0$, we also have the continued fraction

$$\langle\rho\rangle=\cfrac{2}{|p|+\cfrac{4}{|p|+\cfrac{6}{|p|+\cfrac{8}{|p|+\cfrac{}{|p|+\cdots}}}}}$$

Higher moments can be computed directly or by the recursion formula

$$\langle\rho^n\rangle=p\langle\rho^{n-1}\rangle+2(n-1)\langle\rho^{n-2}\rangle.$$

In particular, $\langle\rho^2\rangle=p\langle\rho\rangle+2$ and $\langle(\Delta\rho)^2\rangle=\langle\rho^2\rangle-\langle\rho\rangle^2$ which govern total amplitude noise are plotted in V, Fig. 5 and QVII, Fig. 3 and quoted in Table I of this paper.

TABLE II. Spectrum $S_p(\omega)$ for phase (and amplitude) fluctuations.

Frequency ω	Pump parameter p −10	−2	−1	0	1	2	10[a]
0	0.07429	0.8259	1.420	2.677	5.535	12.18	389.8
0.25	0.07425	0.8205	1.404	2.618	5.274	10.85	367.7
0.5	0.07412	0.8047	1.357	2.457	4.619	8.179	314.4
1.0	0.07361	0.7474	1.199	1.971	3.088	4.128	199.0
2.0	0.07163	0.5816	0.8188	1.101	1.333	1.400	80.61
5.0	0.06029	0.2281	0.2551	0.2723	0.2751	0.2636	15.62
10.0	0.03852	0.07222	0.07438	0.07522	0.07460	0.07258	4.033
20.0	0.01576	0.01943	0.01956	0.01959	0.01951	0.01930	1.024
50.0	0.003068	0.003184	0.003187	0.003188	0.003185	0.003178	0.1721
100.0	0.0007916	0.0007990	0.0007992	0.0007992	0.0007990	0.0007986	0.04870

[a] For $p=10$ the correct frequency is $\frac{1}{10}$th the tabulated frequency.

be written

$$\frac{1}{2}\int_{-\infty}^{\infty}\frac{S_a(\omega)\,d\omega}{2\pi}=\langle(\Delta\rho)^2\rangle\equiv\langle\rho^2\rangle-\langle\rho\rangle^2. \quad (5.5)$$

The results[27] for $\bar{\rho}$ and $\langle(\Delta\rho)^2\rangle$ are summarized in Table I.

6. CALCULATION OF THE POWER SPECTRA

The time integrals in Eq. (4.1) and (4.2) suggest that we need not compute $\hat{R}$, which obeys a partial differential equation, rather only its one-sided Fourier transform.

$$G(r, r_0; \lambda, \omega)\equiv\int_0^{\infty} dt\, e^{-i\omega t}\hat{R}(r, t\mid r_0, 0; \lambda). \quad (6.1)$$

The equation obeyed by G may be obtained by taking the one-sided Fourier transform of both sides of Eq. (4.6).

$$\int_0^{\infty} dt\, e^{-i\omega t}\frac{\partial\hat{R}}{\partial t}=\left[H_r-\frac{\lambda^2}{r^2}\right]G(r, r_0; \lambda, \omega). \quad (6.2)$$

The left-hand side of the above equation may be integrated by parts to give an inhomogeneous *ordinary* differential equation for G:

$$\frac{d^2G}{dr^2}+(r^3-pr-r^{-1})\frac{dG}{dr}+\left[3r^2-p+\frac{(1-\lambda^2)}{r^2}-i\omega\right]G$$
$$=-\hat{R}(r, 0\mid r_0, 0; \lambda)=-\delta(r-r_0) \quad (6.3)$$

of the Green's-function form.

We define $U(r)$ to be the homogeneous solution to the above equation which satisfies the boundary condition for G at $r=0$, and we define $V(r)$ to be the homogeneous solution which satisfies the boundary condition for G at $r=\infty$. The solution, $G(r, r_0; \lambda, \omega)$, may be written in terms of $U(r)$ and $V(r)$:

$$G(r, r_0)=-[U(r)V(r_0)/W(r_0)], \quad r\leq r_0$$
$$=-[U(r_0)V(r)/W(r_0)], \quad r\geq r_0 \quad (6.4)$$

where $W(r_0)$ is the Wronskian

$$W(r)=U(r)V'(r)-V(r)U'(r)$$
$$=Ar\exp(-\tfrac{1}{4}r^4+\tfrac{1}{2}pr^2), \quad (6.5)$$

where A is a constant. We notice that the Wronskian is just a constant times the steady-state amplitude probability distribution $P(r)$.

The spectra $S_p(\omega)$ and $S_a(\omega)$ can now be computed directly from $G(r, r_0; \lambda, \omega)$ by the following integrations:

$$S_p(\omega)=4\,\mathrm{Re}\int_0^{\infty} dr_0 r_0 P(r_0)\int_0^{\infty} dr\, rG(r, r_0; 1, \omega)$$

$$S_a(\omega)=4\,\mathrm{Re}\int_0^{\infty} dr_0(r_0^2-\bar{\rho})\,P(r_0)$$
$$\times\int_0^{\infty} dr(r^2-\bar{\rho})G(r, r_0; 0, \omega). \quad (6.6)$$

Equation (6.6) displays the subtraction of the δ function at $\omega=0$ in the amplitude spectra, which corresponds

TABLE III. Spectrum $S_a(\omega)$ for intensity fluctuations.

Frequency ω	Pump parameter p −10	−2	−1	0	1	2	4	6	8	10
0	0.006680	0.1571	0.2791	0.4966	0.8260	1.158	1.101	0.7122	0.5174	0.4053
1.0	0.006665	0.1546	0.2729	0.4817	0.7945	1.110	1.075	0.7059	0.5151	0.4042
2.0	0.006622	0.1477	0.2561	0.4421	0.7133	0.9878	1.002	0.6878	0.5084	0.4010
5.0	0.006336	0.1123	0.1792	0.2817	0.4201	0.5686	0.6956	0.5847	0.4663	0.3798
10.0	0.005489	0.06079	0.08718	0.1249	0.1763	0.2395	0.3543	0.3860	0.3606	0.3198
15.0	0.004489	0.03459	0.04736	0.06578	0.09188	0.1263	0.2025	0.2502	0.2627	0.2534
20.0	0.003577	0.02163	0.02902	0.03985	0.05557	0.07697	0.1284	0.1692	0.1911	0.1967
30.0	0.002263	0.01048	0.01384	0.01886	0.02631	0.03673	0.06354	0.08888	0.1082	0.1204
50.0	0.001041	0.003966	0.005193	0.007050	0.009846	0.01383	0.02450	0.03564	0.04573	0.05408
100.0	0.000295	0.001014	0.001323	0.001794	0.002508	0.003533	0.006337	0.009409	0.01241	0.01519

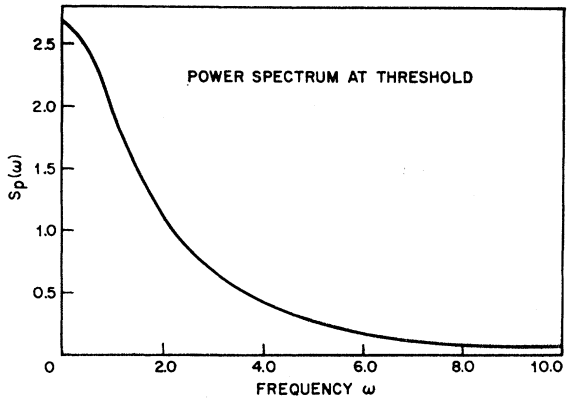

FIG. 2. Power spectrum for phase and amplitude fluctuations $S_p(\omega)$ for the NRWVP oscillator at threshold ($p=0$). The dimensionless frequency ω is given by $\omega=\omega_{exp}\, T$, where T is obtained from Eqs. (A14) or (B13).

to the dc component

$$\bar{\rho}^2=\langle r^2\rangle^2 \quad \text{of} \quad \langle r^2(t)r^2(0)\rangle.$$

To obtain the U and V functions, we must numerically integrate the homogeneous part of the equation for G, Eq. (6.3), with λ, ω, and p treated as parameters. In order to use Numerov's metnod[28] of numerical integration, the first derivative term of Eq. (6.3) must be eliminated by the following transformation on U.

$$U(r)=r^{1/2}\exp(-\tfrac{1}{8}r^4+\tfrac{1}{4}pr^2)u(r) \qquad (6.7)$$

and the same transformation from $V(r)$ to $v(r)$. The resulting differential equation for u (and v) is

$$\frac{d^2u}{dr^2}+\Big[-\tfrac{1}{4}r^6+p\tfrac{1}{2}r^4+(2-\tfrac{1}{4}p^2)r^2-p+i\omega+\frac{(1-4\lambda^2)}{4r^2}\Big]u=0. \qquad (6.8)$$

The question of the power boundary conditions for G at $r=0$ and $r=\infty$ now arises. Since P must be normalized, it must go to zero as r goes to infinity. This is the only boundary condition we have for a second-order equation. Another boundary condition must somehow be imposed at $r=0$. A detailed discussion of the choice of boundary conditions may be found in Appendix C. The results of that appendix are that the least singular solution at $r=0$ is to be taken for $U(r)$, and the exponentially decaying WKB approximation for large r is used to start the numerical integration for V.

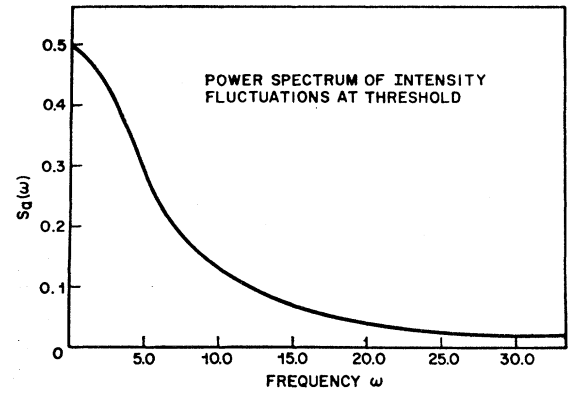

FIG. 3. Power spectrum for amplitude (intensity) fluctuations $S_a(\omega)$ for the NRWVP oscillator at threshold ($p=0$).

[28] A review of this method may be found in D. R. Hartree, *Numerical Analysis* (Oxford University Press, England 1958), Sec. 7.23.

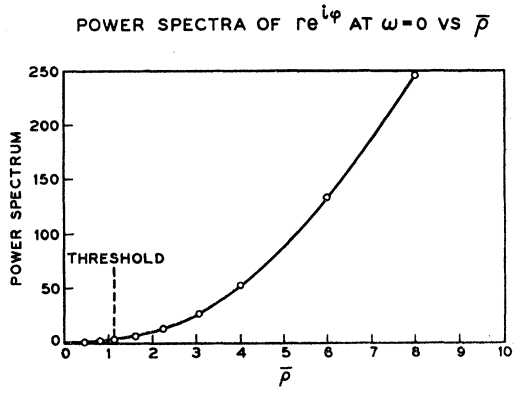

FIG. 4. Height of the power spectrum of phase and amplitude fluctuations $S_p(\omega=0)$ in the NRWVP oscillator versus the mean intensity $\bar{p}$. For lasers this is the normalized maximum of the one-sided Fourier transform of $\langle b^\dagger(t)b(0)\rangle$ plotted versus $\langle b^\dagger b\rangle/\xi^2$, where $\langle b^\dagger b\rangle$ is the mean number of photons and the scaling parameter ξ^2 is defined in Appendix A.

The power spectrum of phase and amplitude fluctuations $S_p(\omega)$ was computed for the pump parameter p equal to -10, -2, -1, 0, 1, 2, and 10. See Table II. The power spectrum of amplitude fluctuations $S_a(\omega)$ was computed for p equal to -10, -2, -1, 0, 1, 2, 4, 6, 8, and 10. See Table III. When compared to a least-squares fit using a single Lorentzian with adjustable height and width, the power spectra were found to be nearly Lorentzian, with deviations only far out in the wings, i.e., for frequencies large compared to the half-

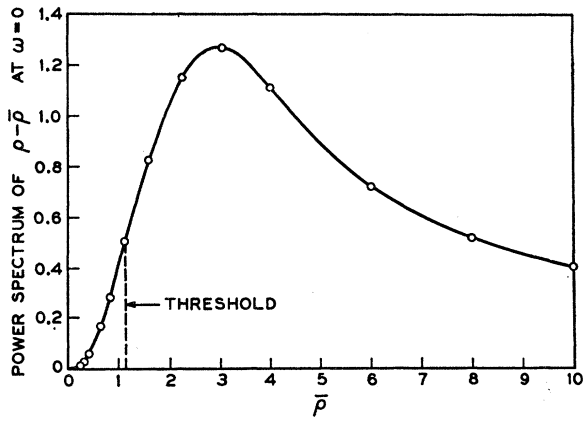

FIG. 5. Height of the power spectrum of amplitude (intensity) fluctuations $S_a(\omega=0)$ for the NRWVP oscillator is plotted versus the mean intensity $\bar{p}$. For lasers this is the maximum of the one-sided Fourier transform of $[\langle b^\dagger(0)b^\dagger(t)b(t)b(0)\rangle-\langle b^\dagger b\rangle^2]/\xi^4$ plotted versus $\langle b^\dagger b\rangle/\xi^2$.

TABLE IV. Ten lowest eigenvalues: phase and amplitude noise.

p	$\Lambda_{1,0}$	$\Lambda_{1,1}$	$\Lambda_{1,2}$	$\Lambda_{1,3}$	$\Lambda_{1,4}$	$\Lambda_{1,5}$	$\Lambda_{1,6}$	$\Lambda_{1,7}$	$\Lambda_{1,8}$	$\Lambda_{1,9}$
−10	10.376	32.858	57.133	82.994	110.293	138.918	168.778	199.798	231.918	265.508
− 2	3.0840	12.889	25.219	39.593	55.721	73.408	92.511	112.292	134.556	157.337
− 1	2.3316	11.008	22.166	35.381	50.359	66.905	84.874	104.157	124.664	146.323
0	1.668	9.400	19.468	31.591	45.480	60.939	77.823	96.021	115.447	136.026
1	1.1206	8.1331	17.186	28.284	41.143	55.568	71.416	88.577	106.963	126.502
2	0.7132	7.299	15.392	25.525	37.411	50.855	65.716	81.885	99.274	117.813
10	0.10212	19.237	27.687	35.064	41.062	47.270	55.227	64.658	75.324	87.111

width at half power. See, for example, Figs. 2 and 3 for the spectra $S_p(\omega)$ and $S_a(\omega)$ at threshold ($p=0$).

To show how these spectra vary with power output, at low frequencies, we show $S_p(\omega)$ and $S_a(\omega)$ at $\omega=0$ in Figs. 4 and 5 plotted against $\bar{p}$ rather than p. We plot against $\bar{p}$ because this variable is more directly accessible to the experimenter than the net pump rate p. Since $\bar{p}=1.128$ at $p=0$ (threshold), the abscissa can be interpreted by the experimentalist to mean

$$\bar{p}=1.128\langle b^\dagger b\rangle/\langle b^\dagger b\rangle_{\text{threshold}}$$
$$=1.128\ (\text{power out})/(\text{threshold power out}). \quad (6.9)$$

7. EIGENFUNCTION EXPANSION

Since the power spectra were found to be nearly Lorentzian, the time dependence of the correlation functions $\langle a^*(t)a(0)\rangle$ and $\langle a^*(0)a^*(t)a(t)a(0)\rangle$ must be dominated by the lowest nonzero eigenvalues of the equation for $\hat{R}$, Eq. (4.6), with $\lambda=1$ and $\lambda=0$, respectively. This suggests that another approach to the spectra can be made by seeking the eigenfunctions of the operator $[H_r-(\lambda^2/r^2)]$:

$$\partial\hat{R}_n/\partial t=[H_r-(\lambda^2/r^2)]\hat{R}_n=-\Lambda_{\lambda,n}\hat{R}_n. \quad (7.1)$$

We assume the same boundary conditions for $\hat{R}_n(r)$ that we found for $G(r, r_0)$ in Appendix C. From Eq. (6.7) we can see that the transformation $\hat{R}_n(r)=[P(r)]^{1/2}Q_n(r)$ transforms the above eigenvalue equation to

$$\left\{\frac{d^2}{dr^2}-\tfrac{1}{4}r^6+\tfrac{1}{2}pr^2+(2-\tfrac{1}{4}p^2)r^2-p+\frac{(1-4\lambda^2)}{4r^2}\right\}Q_n$$
$$=-\Lambda_{\lambda,n}Q_n. \quad (7.2)$$

Using Eq. (7.2) and Numerov's method[28] of numerical integration, the first ten eigenfunctions and the corresponding eigenvalues $\Lambda_{1,n}$ and $\Lambda_{0,n}$ were computed. These eigenvalues are given in Tables IV and V.

The Hermiticity of the operator in braces { } guarantees that its eigenfunctions Q_n obey the unweighted orthogonality[26] condition

$$\int_0^\infty Q_m(r)Q_n(r)\,dr=\delta_{mn}. \quad (7.3)$$

If we assume completeness

$$\sum_n Q_n(r)Q_n(r')=\delta(r-r'), \quad (7.4)$$

we can expand[17] the unnormalized conditional probability $\hat{R}(r, t\mid r_0, 0; \lambda)$:

$$\hat{R}(r, t\mid r_0, 0; \lambda)P(r_0)$$
$$=\sum_n \hat{R}_n(r, \lambda)\hat{R}_n(r_0, \lambda)\exp(-\Lambda_{\lambda,n}t). \quad (7.5)$$

Substituting this expression into our expressions, Eq. (4.1) and Eq. (4.2), for $S_p(\omega)$ and $S_a(\omega)$ we obtain

$$S_p(\omega)=4\sum_{n=0}^{\infty}\frac{\Lambda_{1,n}}{\omega^2+{\Lambda_{1,n}}^2}\left[\int_0^\infty r\hat{R}_n(r, 1)\,dr\right]^2,$$

$$S_a(\omega)=4\sum_{n=1}^{\infty}\frac{\Lambda_{0,n}}{\omega^2+\Lambda_{0,n}}\left[\int_0^\infty r^2\hat{R}_n(r, 0)\,dr\right]^2, \quad (7.6)$$

after making use of the reality[29] of $\hat{R}_n(r, \lambda)$ and $\Lambda_{\lambda,n}$. Note that $S_p(\omega)$ and $S_a(\omega)$ both have peaks at $\omega=0$ but that the observed spectrum is really $S_p(\omega-\omega_0)$ because of the transformation (B4). [A similar transformation in the laser case is made in QIV (6.12).] The intensity-fluctuation spectrum remains $S_a(\omega)$.

TABLE V. Ten lowest nonzero eigenvalues for amplitude fluctuations.

p	$\Lambda_{0,1}$	$\Lambda_{0,2}$	$\Lambda_{0,3}$	$\Lambda_{0,4}$	$\Lambda_{0,5}$	$\Lambda_{0,6}$	$\Lambda_{0,7}$	$\Lambda_{0,8}$	$\Lambda_{0,9}$	$\Lambda_{0,10}$
−10	21.4686	44.8706	69.9541	96.5457	124.516	153.765	184.211	215.786	248.433	282.101
− 2	7.87875	18.9482	32.3125	47.5728	64.4872	82.8880	102.6504	123.676	145.887	169.215
− 1	6.63585	16.4978	28.6881	42.7910	58.5589	75.8210	94.4508	114.349	135.435	157.643
0	5.62661	14.3627	25.4521	38.4612	53.1393	69.3145	86.8594	105.674	125.679	146.806
1	4.92840	12.6035	22.6637	34.6420	48.2869	63.4268	79.9346	97.7109	116.676	136.762
2	4.63584	11.2857	20.3871	31.3963	44.0638	58.2196	73.7376	90.5198	108.487	127.572
4	5.69759	10.2361	17.6572	26.9004	37.7745	50.1112	63.7894	78.7141	94.8086	112.009
6	9.44989	11.5823	18.0587	25.6136	34.8815	45.5776	57.5878	70.8197	85.1997	100.666
8	14.6507	14.9666	23.6663	28.3892	36.2892	45.3983	55.8580	67.5238	80.3198	94.1834
10	19.1140	19.1235	34.5180	35.3941	44.4958	50.7800	59.7451	69.8125	81.0688	93.3982

[29] If our oscillator had been detuned, the eigenfunctions $\hat{R}_n(r, \lambda)$ and the eigenvalues $\Lambda_{\lambda,n}$ would not have been real. Equation (7.6) would then be replaced by a slightly more general equation. [See M. Lax, in *Tokyo Summer Lectures in Theoretical Physics, 1966* (W. A. Benjamin, Inc., New York, 1967), Sec. 22.] See also Ref. 17.

TABLE VI. Fractional contribution $p_{1,n}$ of nth mode to integrated spectrum for amplitude and phase fluctuations.

p	$p_{1,0}$	$p_{1,1}$	$p_{1,2}$	$p_{1,3}$	$p_{1,4}$	$p_{1,5}$	$p_{1,6}$	$p_{1,7}$	$p_{1,8}$	$p_{1,9}$
−10	1.0000	0.1347×10^{-3}	0.8812×10^{-6}	0.1185×10^{-9}	0.8204×10^{-14}	0.1100×10^{-12}	0.6912×10^{-13}	0.5155×10^{-13}	0.4034×10^{-13}	0.3446×10^{-13}
− 2	0.9953	0.4584×10^{-2}	0.4790×10^{-4}	0.6263×10^{-6}	0.9144×10^{-8}	0.1458×10^{-9}	0.2175×10^{-11}	0.7726×10^{-13}	0.1714×10^{-14}	0.4225×10^{-14}
− 1	0.9921	0.7801×10^{-2}	0.1223×10^{-3}	0.2222×10^{-5}	0.4312×10^{-7}	0.8781×10^{-9}	0.1787×10^{-10}	0.4416×10^{-12}	0.2112×10^{-14}	0.4059×10^{-14}
0	0.9867	0.1281×10^{-1}	0.3051×10^{-3}	0.7730×10^{-5}	0.2002×10^{-6}	0.5241×10^{-8}	0.1368×10^{-9}	0.3770×10^{-11}	0.7441×10^{-13}	0.7770×10^{-14}
1	0.9810	0.1923×10^{-1}	0.7066×10^{-3}	0.2518×10^{-4}	0.8707×10^{-6}	0.2943×10^{-7}	0.9747×10^{-9}	0.3214×10^{-10}	0.9842×10^{-12}	0.3954×10^{-13}
2	0.9739	0.2469×10^{-1}	0.1411×10^{-2}	0.7236×10^{-4}	0.3350×10^{-5}	0.1465×10^{-6}	0.6144×10^{-8}	0.2490×10^{-9}	0.9757×10^{-10}	0.4056×10^{-12}
10	0.9950	0.4829×10^{-2}	0.7023×10^{-6}	0.1337×10^{-3}	0.5552×10^{-5}	0.8599×10^{-5}	0.2167×10^{-5}	0.5180×10^{-6}	0.1018×10^{-6}	0.1766×10^{-7}

TABLE VII. Fractional contribution $p_{0,n}$ of nth mode to integrated intensity spectrum.

p	$p_{0,1}$	$p_{0,2}$	$p_{0,3}$	$p_{0,4}$	$p_{0,5}$	$p_{0,6}$	$p_{0,7}$	$p_{0,8}$	$p_{0,9}$	$p_{0,10}$
−10	0.9990	0.9470×10^{-3}	0.1495×10^{-5}	0.3354×10^{-8}	0.7251×10^{-11}	0.1294×10^{-12}	0.1531×10^{-13}	0.1023×10^{-13}	0.7600×10^{-14}	0.4185×10^{-14}
− 2	0.9765	0.2294×10^{-1}	0.4965×10^{-3}	0.1049×10^{-4}	0.2203×10^{-6}	0.4627×10^{-8}	0.9751×10^{-10}	0.2033×10^{-11}	0.4414×10^{-13}	0.3690×10^{-14}
− 1	0.9617	0.3709×10^{-1}	0.1167×10^{-2}	0.3374×10^{-4}	0.9325×10^{-6}	0.2509×10^{-7}	0.6615×10^{-9}	0.1725×10^{-10}	0.4657×10^{-12}	0.9939×10^{-14}
0	0.9370	0.6013×10^{-1}	0.2762×10^{-2}	0.1094×10^{-3}	0.3988×10^{-5}	0.1375×10^{-6}	0.4560×10^{-8}	0.1468×10^{-9}	0.4603×10^{-11}	0.1525×10^{-12}
1	0.8960	0.9724×10^{-1}	0.6512×10^{-2}	0.3538×10^{-3}	0.1699×10^{-4}	0.7508×10^{-6}	0.3129×10^{-7}	0.1244×10^{-8}	0.4821×10^{-10}	0.1789×10^{-11}
2	0.8284	0.1553	0.1508×10^{-1}	0.1120×10^{-2}	0.7073×10^{-4}	0.4003×10^{-5}	0.2092×10^{-6}	0.1030×10^{-7}	0.4821×10^{-9}	0.2166×10^{-10}
4	0.5926	0.3344	0.6343×10^{-1}	0.8629×10^{-2}	0.9308×10^{-3}	0.8563×10^{-4}	0.7036×10^{-5}	0.5218×10^{-6}	0.3613×10^{-7}	0.2361×10^{-8}
6	0.4061	0.4459	0.1133	0.2871×10^{-1}	0.5130×10^{-2}	0.7515×10^{-3}	0.9465×10^{-4}	0.1057×10^{-4}	0.1072×10^{-5}	0.1005×10^{-6}
8	0.4423	0.4622	0.4930×10^{-1}	0.3443×10^{-1}	0.9195×10^{-2}	0.2147×10^{-2}	0.4093×10^{-3}	0.6750×10^{-4}	0.9905×10^{-5}	0.1319×10^{-5}
10	0.4666	0.4832	0.2118×10^{-1}	0.2558×10^{-1}	0.3618×10^{-2}	0.2013×10^{-2}	0.5580×10^{-3}	0.1376×10^{-3}	0.2902×10^{-4}	0.5445×10^{-5}

TABLE VIII. Lowest nonvanishing eigenvalues $\Lambda_a=\Lambda_{0,1}$, $\Lambda_p=\Lambda_{1,0}$ appropriate to intensity and phase fluctuations, respectively.

$\bar{p}$	Λ_a	Λ_p
−10	21.47	10.376
− 9	19.61	9.412
− 8	17.77	8.456
− 7	15.96	7.509
− 6	14.19	6.574
− 5	12.48	5.657
− 4	10.84	4.763
− 3	9.295	3.901
− 2	7.879	3.084
− 1	6.636	2.332
0	5.627	1.668
1	4.928	1.1206
2	4.636	0.7132
3	4.856	0.4489
4	5.698	0.3003
5	7.237	0.2221
6	9.450	0.1780
7	12.08	0.1495
8	14.65	0.1293
9	16.96	0.1141
10	19.11	0.1021

At $t=0$, Eq. (7.5) reduces to

$$\sum_n \hat{R}_n(r,\lambda)\hat{R}_n(r_0,\lambda)=\delta(r-r_0)P(r_0), \quad (7.7)$$

so that

$$\sum_n \int_0^\infty r\hat{R}_n(r,1)\,dr \int_0^\infty r_0\hat{R}_n(r_0,1)\,dr_0 = \int_0^\infty r_0^2 P(r_0)\,dr_0=\bar{p}. \quad (7.8)$$

Similarly, by adding and subtracting the $n=0$ term,

$$\sum_{n\neq 0}\left[\int_0^\infty r^2\hat{R}_n(r,0)\,dr\right]=\langle\rho^2\rangle-\bar{p}^2=\langle(\Delta\rho)^2\rangle. \quad (7.9)$$

Thus, we can rewrite (7.6) in the form

$$S_p(\omega)=4\bar{p}\sum_{n=0}^{\infty}\frac{\Lambda_{1,n}}{\Lambda_{1,n}^2+\omega^2}p_{1,n}, \quad (7.10)$$

$$S_a(\omega)=4\langle(\Delta\rho)^2\rangle\sum_{n=1}^{\infty}\frac{\Lambda_{0,n}}{\Lambda_{0,n}^2+\omega^2}p_{0,n}, \quad (7.11)$$

where

$$p_{1,n}=\left[\int_0^\infty r\hat{R}_n(r,1)\,dr\right]^2\Big/\bar{p},$$

$$p_{0,n}=\left[\int_0^\infty r^2\hat{R}_n(r,0)\,dr\right]^2\Big/\langle(\Delta\rho)^2\rangle, \quad (7.12)$$

are given in Tables VI and VII for a range of values of $\bar{p}$.

The relationships (7.8) and (7.9) guarantee that

$$\sum_{n=0}^{\infty}p_{1,n}=1, \qquad \sum_{n=1}^{\infty}p_{0,n}=1. \quad (7.13)$$

In view of (5.4) and (5.5), we see that $p_{1,n}$ and $p_{0,n}$ represent the fractional contribution of the nth mode to the integrated spectrum of $S_p(\omega)$ and $S_a(\omega)$, respectively.

In the calculation of the power spectra of the preceding section, we found that these spectra were nearly Lorentzian. One possible explanation is that

$$p_{1,n}\ll p_{1,0} \qquad n\geq 1$$
$$p_{0,n}\ll p_{0,1} \qquad n\geq 2. \quad (7.14)$$

Since these coefficients $p_{\lambda,n}$ are all positive, we can get upper and lower bounds for these spectra:

$$S_p{}^l(\omega)\leq S_p(\omega)\leq S_p{}^u(\omega)$$
$$S_a{}^l(\omega)\leq S_a(\omega)\leq S_a{}^u(\omega), \quad (7.15)$$

where

$$S_p{}^l(\omega)\equiv p_{1,0}4\bar{p}\Lambda_p/(\Lambda_p{}^2+\omega^2), \quad (7.16)$$

$$S_a{}^l(\omega)\equiv p_{0,1}4\langle(\Delta\rho)^2\rangle\Lambda_a/(\Lambda_a{}^2+\omega^2), \quad (7.17)$$

$$\Lambda_p=\Lambda_{1,0}; \qquad \Lambda_a=\Lambda_{0,1}. \quad (7.18)$$

Our simpler upper bounds are valid only up to a frequency equal to a geometric mean between the lowest (nonvanishing) eigenvalue and the next larger eigenvalue:

$$S_p{}^u(\omega)=4\bar{p}\Lambda_p/(\Lambda_p{}^2+\omega^2), \qquad \omega^2\leq\Lambda_{1,0}\Lambda_{1,1} \quad (7.19)$$

$$S_a{}^u(\omega)=4\langle(\Delta\rho)^2\rangle\Lambda_a/(\Lambda_a{}^2+\omega^2), \qquad \omega^2\leq\Lambda_{0,1}\Lambda_{0,2}. \quad (7.20)$$

A good estimate of the width of the spectra $S_p(\omega)$ is given by Λ_p. A plot of Λ_p versus $\bar{p}$ is given in Fig. 6, and a tabulation versus $\bar{p}$ is given in Table VIII. A plot of Λ_a versus $\bar{p}$ is compared with the quasilinear estimate of the linewidth of $S_a(\omega)$ (discussed in V) in Fig. 7 and Λ_a is tabulated versus $\bar{p}$ in Table VIII.

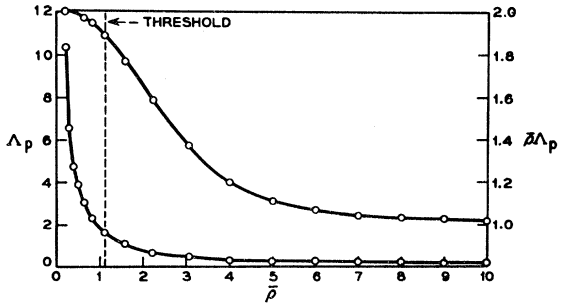

FIG. 6. The lower curve is the half-width at half power Λ_p of the Lorentzian that is a close approximation to the power spectrum of phase and amplitude fluctuations in the NRWVP oscillator versus the dimensionless intensity $\bar{p}$. For lasers this is approximately the half-width at half-maximum of the one-sided Fourier transform of $\langle b^\dagger(t)b(0)\rangle$ plotted in dimensionless form $\Lambda_p=\frac{1}{2}W_pT$ against the dimensionless number of photons $\bar{p}$, where p and T are defined in Appendix A. The upper curve is $\bar{p}$ times the half-width, which shows the transition in the threshold region between the value 2 below threshold predicted correctly by mean value methods and the value 1 above threshold predicted correctly by the quasilinear approximation.

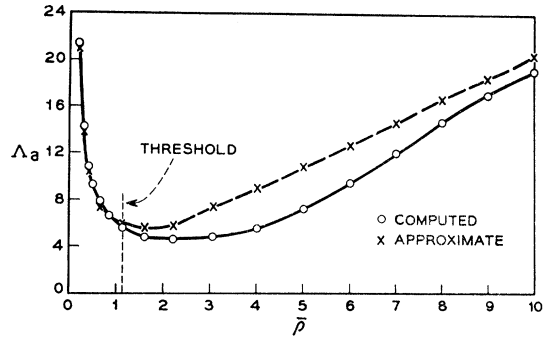

FIG. 7. Half-width at half power Λ_a of the Lorentzian that is a close approximation to the power spectrum of amplitude (intensity) fluctuations in the NRWVP oscillator versus the dimensionless pump parameter $\bar{p}$. For lasers this is approximately the half-width at half maximum of the one-sided Fourier transform of $\langle b^\dagger(0)b^\dagger(t)b(t)b(0)\rangle - \langle b^\dagger b\rangle^2$ plotted in dimensionless form $\Lambda_a = \frac{1}{2}W_a T$ versus the net pump rate $\bar{p}$, where T and $\bar{p}$ are defined in Appendix A.

A comparison of $S_p{}^u(\omega)$ with $S_p(\omega)$ demonstrates close agreement (within 3% at all operating levels. For amplitude noise similar agreement between $S_a{}^u(\omega)$ and $S_a(\omega)$ is obtained except in the region (roughly) of $2 \leq p \leq 6$ where differences as large as 20% were observed.[30]

This complexity arises from the asymptotic degeneracy of the lowest nonzero eigenvalue for amplitude fluctuations as the pump parameter becomes positive and infinite.[31] This degeneracy may be best understood by considering the analogy to a one-dimensional Schrödinger equation with the potential

$$V = \tfrac{1}{4}r^6 - \tfrac{1}{2}pr^4 + (\tfrac{1}{4}p^2 - 2)r^2 + p - \tfrac{1}{4}r^{-2}. \quad (7.21)$$

For negative p this potential is just a single well, however for positive p a bump in the well appears, hereafter referred to as the potential barrier. The height of this barrier is an increasing function of p so that as p becomes positive and infinite the potential transforms into two wells. It is well known that the eigenvalues of a double-well potential are doubly degenerate. We expect and find that as the height of the barrier approaches the lowest nonzero eigenvalue, this eigenvalue becomes nearly degenerate. To demonstrate this we plot in Fig. 8 the potential for p equal to 0 (threshold, no near degeneracies), +6 (height of potential barrier is just above the lowest nonzero eigenvalue), and +10 (lowest-four nonzero eigenvalues are below the height of the barrier and are nearly pairwise degenerate). The four lowest nonzero eigenvalues for each value of p are plotted as horizontal lines above the corresponding outer wells. In Fig. 9 we plot the height of the barrier

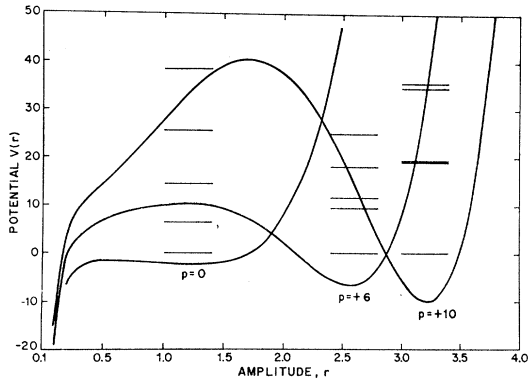

FIG. 8. The curves are the potentials for amplitude fluctuations [defined by (7.21)] for the dimensionless pump parameter p equal to 0 (threshold of oscillation, no near degeneracies), +6 (height of barrier just above lowest nonzero eigenvalue), and +10 (two pairs of nearly degenerate eigenvalues). The lines above each of the outer potential wells give the values of the four lowest nonzero eigenvalues for the corresponding values of the pump parameter p in addition to the steady-state (zero) eigenvalue.

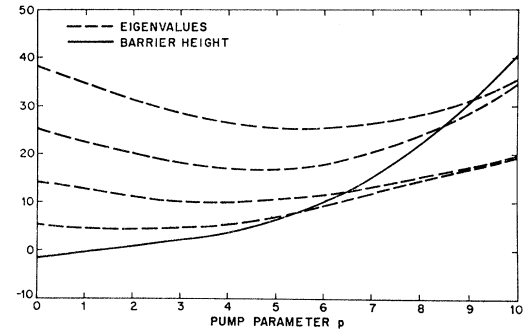

FIG. 9. The solid curve is the height of the barrier in the potential for amplitude fluctuations plotted versus the dimensionless pump parameter p for operation above threshold. The dashed curves are the four lowest nonzero eigenvalues. As the height of the barrier approaches the lowest nonzero eigenvalue, it becomes nearly degenerate with the second lowest nonzero eigenvalue, and similarly for successively higher pairs of eigenvalues.

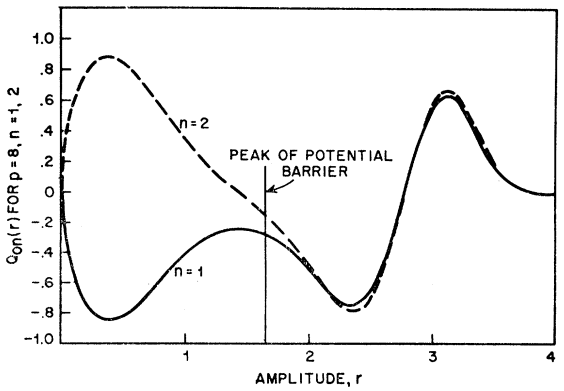

FIG. 10. The two lowest amplitude eigenfunctions $Q_{0,n}(r)$ for $n=1, 2$ of Eq. (7.2) are plotted versus r for $p=8$. This is sufficiently far above threshold for these eigenfunctions to be nearly degenerate. The wave functions agree to the right of the potential barrier and are out of phase to the left of the potential barrier.

[30] By comparing $\int r^2 \hat{R}_1(r, 0)dr$, with $\langle(\Delta\rho)^2\rangle$ using variationally selected wave functions, Risken found that the lowest mode, in the amplitude case, did not supply almost all of the total fluctuation. The work to be described below explains the importance of the lowest two modes in the region $p > 2$.

[31] The existence of this degeneracy was emphasized by W. Lamb, Jr. (private communication).

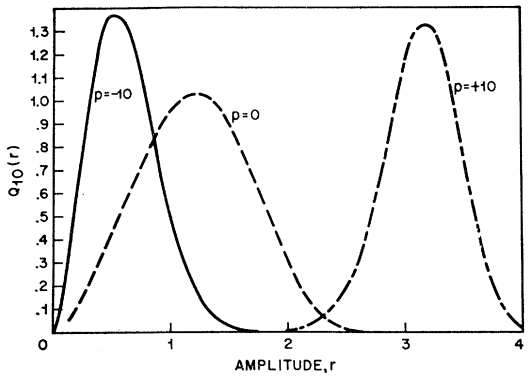

FIG. 11. The lowest eigenfunction $Q_{1,0}(r)$ of (7.2) appropriate to phase fluctuations is plotted versus r for $p=-10$ (well below threshold), $p=0$ (at threshold) and $p=10$ (well above threshold)

as a function of p and the four lowest nonzero eigenvalues as a function of p. The continuous approach to near pairwise degeneracy and its correlation with the height of the barrier is clearly shown by this graph. It is only the near degeneracy of the lowest nonzero eigenvalue which is important to us here, since dominant contributions to the power spectrum by the *two* lowest nonzero eigenvalues will still yield a nearly Lorentzian power spectrum.

The eigenfunctions $Q_{0,n}(r)$ for $n=1$, 2 are shown in Fig. 10 for $p=8$ a case in which an appreciable barrier exists. These eigenfunctions agree near the peak $r\approx(\bar{p})^{1/2}\approx p^{1/2}$ but are out of phase near the peak at $r=0$. After multiplication by $[P(r)]^{1/2}$ to obtain $\hat{R}_n(r, 0)$ the peak at $(\bar{p})^{1/2}$ is accentuated and that near $r=0$ becomes unimportant. This is why the contribution of the $n=1$ and $n=2$ modes to amplitude noise becomes nearly equal for large p, as shown in Table V. For phase noise, we show in Fig. 11 $Q_{1,n}(r)$ for $n=0$ and $p=-10$, 0 and 10, i.e., well below, at, and well above threshold. The peak at $(\bar{p})^{1/2}$ asserts itself as we move well above threshold.

8. ACCURACY OF COMPUTATIONS

When the power spectra computed by the Green's-function method of Sec. 6 were compared to the results of the eigenfunction method, discrepancies were found. The differences were of the order of 0.5% for phase and amplitude fluctuations and 2% for amplitude fluctuations. By using the same two methods to compute the (known) power spectra for a harmonic oscillator, the errors in the Green's function calculations were approximately the same as the percentage differences given above. On the other hand, the eigenfunction method was accurate to 0.01%. These relative accuracies could have been anticipated since the numerical integrations required in the Green's-function method introduce greater numerical errors than the moment integrations of the eigenfunction method. Furthermore, the larger errors of the Green's-function calculation of the power spectra for amplitude fluctuations, than for the Green's-function calculation of the power spectra for phase and amplitude fluctuations, are a result of the delicate subtraction of the δ function in the former calculation. The rapid oscillation of the eigenfunctions with more than ten nodes guarantees that the truncation of the summation in Eq. (7.6) at $n=10$ introduces a much smaller error than the numerical errors in the computation of the first ten moments. Thus, we expect that the errors in the power spectra calculated by the eigenfunction method are less than one part in 10^4, since the power spectra in the harmonic oscillator were calculated to this accuracy. The values that we quoted in Tables II and III for the power spectra are those computed by the eigenfunction method.

9. SUMMARY

An examination of Fig. 7 shows that outside the region $-10\leq p\leq 10$ or $0.2\leq\bar{p}\leq 10$ the quasilinear approximation $\Lambda_a\approx(2\bar{p}+4/\bar{p})$ of V (9.16) is an excellent approximation to the linewidth for intensity fluctuations. In Fig. 6 the curve for $\bar{p}\Lambda_p$ varies smoothly from 2 below threshold to 1 above threshold. Thus for $p>10$ ($\bar{p}>10$) the phase linewidth Λ_p is adequately approximated[32] by the quasilinear result V (4.14), (9.15):

$$(\Lambda_p)_{QL}\approx 1/\bar{p}, \tag{9.1}$$

whereas well below threshold ($p<-10$, $\bar{p}<0.2$) the phase linewidth is accurately approximated by the mean-value approximation[32]

$$(\Lambda_p)_{MV}\approx 2/\bar{p} \tag{9.2}$$

of V (7.9) or V (9.15).

Thus we have established that elementary linearization methods work for a self-sustained oscillator outside the threshold region ($-10\leq p\leq 10$). Inside the threshold region, Fokker–Planck methods are needed. In Appendix B, using a circuit model, we have shown that any *well-designed* oscillator will be represented to a good approximation by the rotating-wave Van der Pol oscillator over a broad region including the threshold region. *Thus, in the only region requiring nonlinear techniques the problem has been reduced to the normalized rotating-wave oscillator problem, for which the present paper supplies detailed, accurate numerical solutions.*

A well-designed oscillator is one whose output is sinusoidal rather than periodic, and whose output is large compared to typical thermal fluctuations in positive resistance circuits. In Appendix A we use the description of a gas laser taken from QXII and show explicitly that the RWVP description is valid near threshold. For such an oscillator, the spectrum is nearly sinusoidal, and the criterion of large output is merely that the number of photons at threshold be large compared to unity.

[32] See for example V, QV; Refs. 6, 9.

APPENDIX A: THE LASER MODEL

In QXII, Lax and Louisell study a model for a maser in which the Fokker-Planck equation for the associated classical function $P(\beta, \beta^*, N_1, N_2, t)$ which corresponds dynamically to the density matrix of the electromagnetic field and atomic population variables. The Langevin equations for this Fokker-Planck process are obtained. For a gas laser, the atomic response rates are fast compared to the photon rates so that the population variables N_1 and N_2 follow the instantaneous value of the radiation field. Thus, an adiabatic approximation for the population variables yields a Fokker–Planck equation for the associated classical function $P(\beta, \beta^*, t)$ which corresponds dynamically to the density matrix of the electromagnetic field $\rho(b, b^\dagger, t)$.

The Langevin equations corresponding to the $P(\beta, \beta^*, t)$ Fokker-Planck process are found to have the form

$$d\beta/dt=\tfrac{1}{2}(1-i\alpha)\beta\{-\gamma+\pi[(R_2+\tilde{G}_2)J_2-(R_1+\tilde{G}_1)J_1]\}+\tilde{G}_\beta, \quad \text{(A1)}$$

where α is a measure of the detuning (which we shall set equal to zero in this paper), $R_2=Nw_{20}$ and $R_1=Nw_{10}$ are the pump rates into the upper (2) and lower (1) states, respectively, and

$$J_2=(\Gamma_1-w_{12})/\Delta,$$
$$J_1=(\Gamma_2-w_{21})/\Delta, \quad \text{(A2)}$$
$$\Delta=\Gamma_1\Gamma_2-w_{12}w_{21}+\pi(\Gamma_1+\Gamma_2-w_{12}-w_{21})I, \qquad I\equiv|\beta|^2.$$

The radiative rate constant π is such that the rate of downward transitions are $\pi N_2(I+1)$ whereas the rate of upward transitions are $\pi N_1 I$ where N_2 and N_1 are the upper and lower state populations and $\langle I\rangle=\langle|\beta|^2\rangle=\langle$number of photons$\rangle$. The nonradiative transition rate from $1\leftarrow 2$ is w_{12}. The total decay rate out of state 1 (or 2) excluding the radiative rate to 2 (or 1) is Γ_1 (or Γ_2).

Typical parameters[33] for a gas laser are $\Gamma_1, \Gamma_2\sim 10^8$ sec^{-1}, $\pi\sim(1/10)$ sec^{-1}. From the quasilinear treatment of QVII [(6.5)-(6.7)] and Eq. (A18) below we see that the number of photons at threshold is of order $(\Gamma_2/\pi)^{1/2}$. The nonlinearity in J_1 and J_2 is of the form $(\Gamma_e+\pi I)^{-1}$, where

$$\Gamma_e=(\Gamma_1\Gamma_2-w_{12}w_{21})/(\Gamma_1+\Gamma_2-w_{12}-w_{21}), \quad \text{(A3)}$$

so that near threshold $\pi I\ll\Gamma_e$ and we may expand J_1 and J_2 keeping terms linear in I. In this region, the noise sources $\pi J_2\tilde{G}_2\sim(\pi/\Gamma_e)\tilde{G}_2$ and $\pi J_1\tilde{G}_1$ are entirely negligible. Our Langevin process then reduces to the form

$$d\beta/dt=\tfrac{1}{2}(1-i\alpha)\beta\gamma\{\Pi-R_0|\beta|^2\}+\tilde{G}_\beta, \quad \text{(A4)}$$

where

$$\Pi=\left(\frac{\pi}{\gamma}\right)\frac{R_2(\Gamma_1-w_{12})-R_1(\Gamma_2-w_{21})}{\Gamma_1\Gamma_2-w_{12}w_{21}}-1, \quad \text{(A5)}$$

$$R_0=\left(\frac{\pi}{\gamma}\right)\frac{R_2(\Gamma_1-w_{12})-R_1(\Gamma_2-w_{21})}{\Gamma_1\Gamma_2-w_{12}w_{21}}\times\left(\frac{\pi(\Gamma_1+\Gamma_2-w_{12}-w_{21})}{\Gamma_1\Gamma_2-w_{12}w_{21}}\right), \quad \text{(A6)}$$

and

$$\langle\tilde{G}_\beta(t)^*\tilde{G}_\beta(u)\rangle=2D_{\beta^*\beta}\delta(t-u), \quad \text{(A7)}$$

$$2D_{\beta^*\beta}=\gamma\bar{n}+\pi\bar{N}_2=\gamma\bar{n}+\pi\frac{R_2}{\Gamma_2}\frac{(1+w_{21}R_1/\Gamma_1)}{1-(w_{12}w_{21}/\Gamma_1\Gamma_2)}, \quad \text{(A8)}$$

where $\bar{N}_2$ is the adiabatic value of N_2 and

$$\bar{n}=[\exp(\hbar\omega_0/kT)-1]^{-1} \quad \text{(A9)}$$

describes the blackbody noise of the electromagnetic field at the frequency ω_0 of oscillation.

Under the scale and time transformations

$$\beta=\xi a, \qquad t=T\tau, \quad \text{(A10)}$$

our equation can be made to take the canonical form

$$da/d\tau=(1-i\alpha)a(p-|a|^2)+h(\tau), \quad \text{(A11)}$$

$$\langle h^*(\tau)h(\tau')\rangle=4\delta(\tau-\tau'), \quad \text{(A12)}$$

by choosing

$$\xi^2=(D_{\beta^*\beta}/\gamma R_0)^{1/2}, \quad \text{(A13)}$$
$$T=2(\gamma R_0 D_{\beta^*\beta})^{-1/2}, \quad \text{(A14)}$$
$$p=\tfrac{1}{2}\tau T\Pi. \quad \text{(A15)}$$

All calculations of this paper set $\alpha=0$, i.e., neglect detuning. In Table I we find that $\bar{p}=\langle|a|^2\rangle=1.128$ when $p=0$, so that at threshold $\langle|\beta|^2\rangle=1.128\xi^2$.

To see the order of magnitude of the above expressions, let $w_{12}=w_{21}=R_1=0$, so that

$$\Pi=(R_2/R_t)-1, \quad \text{(A16)}$$

where

$$R_t=\gamma\Gamma_2/\pi \quad \text{(A17)}$$

is the threshold pump rate. Then

$$\xi^2=(\Gamma_e/2\pi)^{1/2}[1+(\bar{n}R_t/R_2)]^{1/2}, \quad \text{(A18)}$$
$$p=2\xi^2[1+(\bar{n}R_t/R_2)]^{-1}[1-(R_t/R_2)]. \quad \text{(A19)}$$

Thus we see that the spectrum associated with $\langle b^\dagger(t)b(0)\rangle$ and the intensity spectrum associated with $\langle b^\dagger(0)b^\dagger(t)b(t)b(0)\rangle-\langle b^\dagger b\rangle^2$ are, aside from scaling factors (ξ^2 and ξ^4, respectively) just the classical spectra associated with $\langle a^*(t)a(0)\rangle$ and $\langle\rho(t)\rho(0)\rangle-\langle\rho\rangle^2$, respectively. Moreover, one can avoid the use of (A15 (A19) if one plots not against pump rate but against $\bar{p}=1.128\langle b^\dagger b\rangle/\langle b^\dagger b\rangle_{\text{thr}}$, i.e., against the number of photons relative to the number at threshold.

[33] See, D. E. McCumber, Phys. Rev. **141**, 306 (1966) and Table 1 of QVII.

To assess the accuracy of our expansion of J_1 and J_2 to linear terms, we compare the ratio of the first neglected terms to the first retained term:

$$(\pi I/\Gamma_e)^2/(\pi I/\Gamma_e)=\pi I/\Gamma_e\approx\rho/(2\xi^2).$$

Since ρ is of order unity in the threshold region, we see that the first neglected term has relative importance $1/\xi^2\sim 1/(\text{number of photons at threshold})$. In a well-designed laser, the number of photons at threshold is large (10^2 or 10^4) and the neglected terms are unimportant.

APPENDIX B: THE CIRCUIT MODEL

We review here a general model of a self-sustained oscillator, and examine the reduction of its equations of motion to the Langevin equation for the normalized rotating-wave Van der Pol (NRWVP) oscillator.[34] While this approach is motivated by the study of laser noise by Lax and Louisell, it is to be viewed as a study of the extent to which the noise analysis of this paper may be applied to other self-sustained oscillators. Specifically, if the equation of motion of a self-sustained oscillator is of the type studied below, with suitable scaling parameters this paper gives the power spectra of the fluctuations in that oscillator for operation near the threshold of oscillation. We will find that the basis for this generality is the relative narrowness of the threshold region, which is analogous to a phase transition.

Let us consider an oscillator that possesses no reactance other than that associated with a tuned circuit, but which contains a nonlinear resistance[35] which is a function of a control parameter D. Using the standard notation for the circuit parameters, the equation of motion is

$$L(dI/dt)+C^{-1}Q+R(D)I=e(t), \qquad \text{(B1)}$$

where $e(t)$ is a fluctuating voltage source assumed to have the following properties:

(1) $e(t)$ is a Gaussian random variable of mean zero, i.e., $\langle e(t)\rangle=0$.

(2) The power spectrum of $e(t)$,

$$\mathrm{Re}4\int_0^\infty \langle e^*(t)e(0)\rangle e^{-i\omega t}dt,$$

is approximately independent of ω for $|\omega-\omega_0|\lesssim 1/\Lambda$, where Λ is a characteristic decay time of the circuit.

We must now examine $R(D)$. The control parameter could depend upon the history of the circuit. While this case is common (e.g., solid-state lasers), we shall treat here only those oscillators for which an adiabatic approximation may be made which will allow us to express D in terms of the *instantaneous* excitation of the circuit.[36] Thus,

$$R[D(t)]\cong R[Q(t), I(t)]. \qquad \text{(B2)}$$

For a high-Q circuit the harmonic content of the output may be neglected. In order to identify this harmonic content we introduce complex amplitudes a and a^*. By analogy with the definition of the creation and annihilation operators of the electromagnetic field, we define a and a^* to be

$$a=I-i\omega_0 Q; \qquad a^*=I+i\omega_0 Q, \qquad \text{(B3)}$$

where ω_0 is the resonant frequency of the circuit. In the absence of fluctuations, a would contain only the negative frequency $-\omega_0$, and a^* would contain only the positive frequency $+\omega_0$. The introduction of fluctuations smears out the power spectra of a and a^* about $-\omega_0$ and $+\omega_0$, respectively. We seek a "pure-spectrum" solution of the form

$$a=A\exp(-i\omega_0 t); \qquad a^*=A^*\exp(+i\omega_0 t), \qquad \text{(B4)}$$

where A and A^* are to be slowly-varying functions of time. We can now expand $R(Q, I)I$ as a polynomial in a and a^* and replace a by $A\exp(-i\omega_0 t)$ and a^* by $A^*\exp(i\omega_0 t)$ to get

$$R(Q, I)I=\tfrac{1}{2}\sum_{n=1}^{\infty}[R_n(|a|^2)(A^*)^n\exp(-in\omega_0 t) + R_n(|a|^2)^*A^n\exp(in\omega_0 t)]. \qquad \text{(B5)}$$

We see from the equation of motion for the circuit Eq. (B1) that A and A^* will be slowly varying only if we neglect terms containing $\exp(-in\omega_0 t)$ and $\exp(in\omega_0 t)$ for $n\geq 2$. Thus, the harmonic content of the output is neglected by taking[37]

$$R(Q, I)I\cong\tfrac{1}{2}R_1(|a|^2)(a+a^*)=R(|a|^2)I, \qquad \text{(B6)}$$

where $R_1(|a|^2)$ is required to be real by the constraint that $R(Q, I)I$ contains no reactive part.

The equation of motion may be further simplified by restricting our attention to the region of operation near threshold. If we make a Taylor-series expansion of the nonlinear resistance about the operating point ρ_0 [see, e.g., V (8.19)] where $\rho\equiv|a|^2$ and neglect all second-order and higher-order terms, we obtain

$$R(\rho)\cong R(\rho_0)+[\partial R(\rho_0)/\partial\rho_0](\rho-\rho_0)=R_0\rho-\Pi, \qquad \text{(B7)}$$

where

$$R_0=[\partial R(\rho_0)/\partial\rho_p]; \qquad \Pi=\rho_0[\partial R(\rho_0)/\partial\rho_0]-R(\rho_0). \qquad \text{(B8)}$$

[34] See V and Ref. 17.

[35] The reactance and the frequency dependence of the resistance (omitted here) were shown in V (3.22) to have the sole effect of introducing a detuning parameter [the α in (A.11)] which couples amplitude and phase fluctuations. Since the numerical work in this paper omits detuning, we can start directly with the Eq. (B.1) rather than the more general V (3.13).

[36] Our results will not depend on the adiabatic approximation, since, in the vicinity of threshold, amplitude and phase fluctuations become slow, so that D will in general be able to follow them instantaneously.

[37] The choice $R(|a|^2)I$ is equivalent to assuming that the nonlinearity depends primarily on the energy stored in the circuit.

In order to make the rotating-wave approximation, we rewrite the equation of motion in terms of the complex variables a and a^*:

$$da/dt+i\omega_0 a+(2L)^{-1}R(\rho)a=(2L)^{-1}R(\rho)a^*+L^{-1}e(t). \tag{B9}$$

Since a contains only frequency components centered about $-\omega_0$, and a^* appears as a driving term which contains frequency components centered about $+\omega_0$, we can neglect the term in a^* for a sufficiently high Q circuit. Therefore, we neglect the coupling between a and a^* by neglecting the term in a^* of the above equation and the term in a of the complex conjugate equation. This "rotating-wave approximation" must in fact be made if we wish the solution to have no harmonic content in the absence of noise.

Substituting our linear approximation for $R(\rho)$ and introducing $A=x-iy$, we obtain Langevin equations in the variables x and y for the rotating-wave Van der Pol (RWVP) oscillator:

$$\begin{aligned} dx/dt&=-[R_0(x^2+y^2)-\Pi]x/2L+F_x \\ dy/dt&=-[R_0(x^2+y^2)-\Pi]y/2L+F_y, \end{aligned} \tag{B10}$$

where[38]

$$F_x(t)\equiv L^{-1}e(t)\cos\omega_0 t; \qquad F_y(t)\equiv -L^{-1}e(t)\sin\omega_0 t. \tag{B11}$$

As for the laser treated in Appendix A, we can introduce a scaling transformation to dimensionless variables:

$$a=\xi a', \qquad t=Tt'. \tag{B12}$$

The scaling can be chosen so that only one parameter p remains in the Langevin equations. This is a measure of the negative resistance in the circuit. By analogy with the laser, it is called the pump parameter. In V (Sec. 9) it is shown that the desired choice for ξ and T is

$$\xi^2=[(e^2)_{\omega_0}/2LR_0]^{1/2}; \qquad T=4L^2\xi^2/(e^2)_{\omega_0}, \tag{B13}$$

where $(e^2)_{\omega_0}$ is the power spectrum of the noise source $e(t)$ evaluated at the resonant frequency. With this transformation, we obtain the NRWVP oscillator Langevin equations given in Eqs. (2.1) and (2.2), where we have dropped the primes. The pump parameter p is defined to be Π/ξ^2, and the new Langevin forces are

$$F_x'=(T/\xi)F_x, \tag{B14}$$

and similarly for F_y'.

[38] Note that the noise sources of (B.11) are those of a nonstationary process. Over a time interval $\Delta t\gg\omega_0^{-1}$ this nonstationary process can be replaced, to an excellent approximation, by a stationary process as discussed in V, Sec. 5. The most relevant portion of the argument is repeated here. The random forces F_x and F_y of (2.1) and (2.2) are those of the "reduced" stationary process whereas those of (B.11) are appropriate to the original process.

We are now in a position to treat the case where the noise source $e(t)$ is not exactly white, i.e., the noise source is not exactly delta correlated. We anticipate that if the power spectrum of the noise source $e(t)$ is a slowly-varying function of frequency, a Markoffian description is approximately valid. We must, therefore, determine the diffusion coefficients. To do this, we calculate $\Delta x\equiv x(t+\Delta t)-x(t)$ in the limit of Δt much less than the relaxation time, $1/\Lambda$, of the circuit with no negative resistance. Thus, following the iterative procedure of Sec. 2, the correlation of the Langevin forces enters only in the calculation of the second-order diffusion coefficients. For example,

$$\langle(\Delta x)_1^2\rangle=\int_t^{t+\Delta t}ds\int_t^{t+\Delta t}ds'\langle F_x(s)F_x(s')\rangle. \tag{B15}$$

Substituting our definition for F_x in terms of the noise source $e(t)$, Eq. (B11), and introducing the power spectrum $(e^2)_\omega$ of $e(t)$, we obtain

$$\langle(\Delta x)_1^2\rangle=\frac{1}{L^2}\int_{-\infty}^{\infty}d\omega(e^2)_\omega\int_t^{t+\Delta t}ds\int_t^{t+\Delta t}ds' \times\exp[i\omega(s-s')]\tfrac{1}{2}\{\cos[\omega_0(s-s')]+\cos[\omega_0(s+s')]\}. \tag{B16}$$

As shown in V (4.10) and V (4.11), the rapidly oscillating term $\cos[\omega_0(s+s')]$ yields a negligible contribution if we choose Δt large compared to the period of the oscillation, i.e., $\omega_0\Delta t\gg 1$. With this Δt, the first term yields

$$\langle(\Delta x)_1^2\rangle=\frac{1}{L^2}\int_{-\infty}^{\infty}d\omega(e^2)_\omega\left\{\frac{\sin^2[\frac{1}{2}(\omega+\omega_0)\Delta t]}{(\omega+\omega_0)^2}+\frac{\sin^2[\frac{1}{2}(\omega-\omega_0)\Delta t]}{(\omega-\omega_0)^2}\right\}. \tag{B17}$$

We see that if we can choose a Δt such that $(\omega_0)^{-1}\ll\Delta t\ll\Lambda^{-1}$ and if the spectrum $(e^2)_\omega$ is nearly constant for frequencies within Λ of the resonant frequency, then the term in the brackets { } of Eq. (B17) may be replaced by

$$\{\ \}\rightarrow\tfrac{1}{2}\pi\Delta t[\delta(\omega+\omega_0)+\delta(\omega-\omega_0)], \tag{B18}$$

and we obtain

$$D_{xx}=\langle(\Delta x)_1^2\rangle/2\Delta t=(e^2)_{\omega_0}/4L^2. \tag{B19}$$

By similar methods, discussed in V, we obtain $D_{yy}=D_{xx}$ and $D_{xy}=0$. These are exactly the results that we would have obtained if we had assumed a pure white-noise source with a power spectrum $(e^2)_{\omega_0}$. This white noise value (B19) is to be expected since we are exciting a resonant circuit so that only the frequency components of the noise source within the natural bandwidth Λ of the resonant frequency will be important in exciting the circuit. Thus, if the power spectrum of the noise source is approximately constant over that range of

frequencies, it must be a good approximation to replace our noise source by white noise with a constant power spectrum equal to the real noise source power spectrum *evaluated at the resonant frequency.*

From these diffusion coefficients we see that the Langevin forces for the "reduced"[38] NRWVP oscillator have just those correlations given in Eq. (2.3).

To see the generality of this procedure, we return to the truncated power-series expansion of Eq. (B7). The next term in the expansion would be the second-derivative term. The ratio of the second-derivative term to the first-derivative term is

$$(\rho-\rho_0)[\partial^2 R(\rho_0)/\partial\rho_0^2]/[\partial R(\rho_0)/\partial\rho_0]. \quad \text{(B20)}$$

In general, our nonlinear resistance has a form

$$R(\rho)=Kf(\rho/\rho_1), \quad \text{(B21)}$$

where ρ_1 is a measure of the range of variation in ρ required to produce an appreciable change in $R(\rho)$, and $f(x)$, $f'(x)$ and $f''(x)$ are all of order unity. Our error is then of order

$$(\rho-\rho_0)/\rho_1=(\Delta\rho)/\rho_1\sim[\langle(\Delta\rho)^2\rangle]^{1/2}/\rho_1\equiv\rho_n/\rho_1, \quad \text{(B22)}$$

where ρ_n is a noise fluctuation in ρ. In a well-designed oscillator, the typical operating level, which is of order ρ_1, is made large compared to the noise ρ_n .Thus the error due to neglecting second-derivative terms, ρ_n/ρ_1, will usually be small.

APPENDIX C: THE BOUNDARY CONDITION FOR $G(r, r_0; \lambda, \omega)$

The only condition we have for a second-order equation is that the probability distribution be normalized. This implies that we choose the least-singular solution at $r=0$ and $r=\infty$. To do this, we must determine the asymptotic behavior of the two linearly independent homogeneous solutions to the equation for U (and V) for small r and for large r. For convenience, we define the coefficient of u on the right-hand side of Eq. (6.8) to be

$$q\equiv-\tfrac{1}{4}r^6+\tfrac{1}{2}(pr^4)+(2-\tfrac{1}{4}p^2)r^2-p-i\omega+(1-4\lambda^2)/4r^2. \quad \text{(C1)}$$

For small r, we may approximate q by

$$q\cong-p-i\omega+(1-4\lambda^2)/4r^2. \quad \text{(C2)}$$

With this approximation for q, the equation for u, Eq. (6.8), may be put into the form of Bessel's equation by the following transformations. We first transform to a new dependent variable

$$T=u/r^{1/2}. \quad \text{(C3)}$$

The equation for T is

$$(d^2T/dr^2)+r^{-1}(dT/dr)+(-p-i\omega-(\lambda^2/r^2))T=0. \quad \text{(C4)}$$

If we now scale the independent variable r by the following transformation

$$z=\beta r, \quad \text{(C5)}$$

where

$$\beta=(p^2+\omega^2)^{1/4}\exp[\tfrac{1}{2}i\tan^{-1}(\omega/p)] \quad \text{(C6)}$$

we obtain Bessel's equation of order λ. Thus, the two linearly independent solutions for a small r are

$$U_1=rJ_\lambda(\beta r); \qquad U_2=rY_\lambda(\beta r). \quad \text{(C7)}$$

For phase and amplitude fluctuations ($\lambda=1$), we find that one solution, U_1, goes to zero and the other solution U_2 goes to a finite, nonzero constant as r goes to zero. For amplitude fluctuations, ($\lambda=0$), both U_1 and U_2 go to zero as r goes to zero. In both cases we take the least-singular solution, namely U_1. For phase and amplitude fluctuations this is equivalent to assuming that the probability distribution in rectangular coordinates, x and y, is finite at the origin. For amplitude fluctuations, this is equivalent to assuming that the probability distribution in the amplitude-squared coordinate ρ is finite at the origin.

For large r, the WKB approximation is valid:

$$v_\pm(r)=[q(r)]^{-1/4}\exp\left[\pm\int^r[q(r')]^{1/2}dr'\right]. \quad \text{(C8)}$$

We take the least-singular solution $v_-(r)$. This is consistent with our detailed-balance condition in Sec. 5.

Since a similar choice of boundary conditions is necessary for the harmonic oscillator, our ability to calculate the (known) power spectra for the harmonic oscillator using the same method (and machine program) confirms the validity of our choice of boundary conditions.